Direccionalidad de los fotorreceptores, su función en visión y en diagnósticos

Understanding photoreceptor directionality in vision and diagnostics

Brian Vohnsen
Advanced Optical Imaging Group
University College Dublin, Irlanda

Structure and optics of the human eye

Cornea
~ 43 dioptres
~ 1.376 refractive index

Lens
~ 18 dioptres
~ Graded index 1.37-1.42

Axial length
22 – 25 mm (or higher)

Retina
~ 70%
~ 6M cones (S,M,L)
~ 90M rods

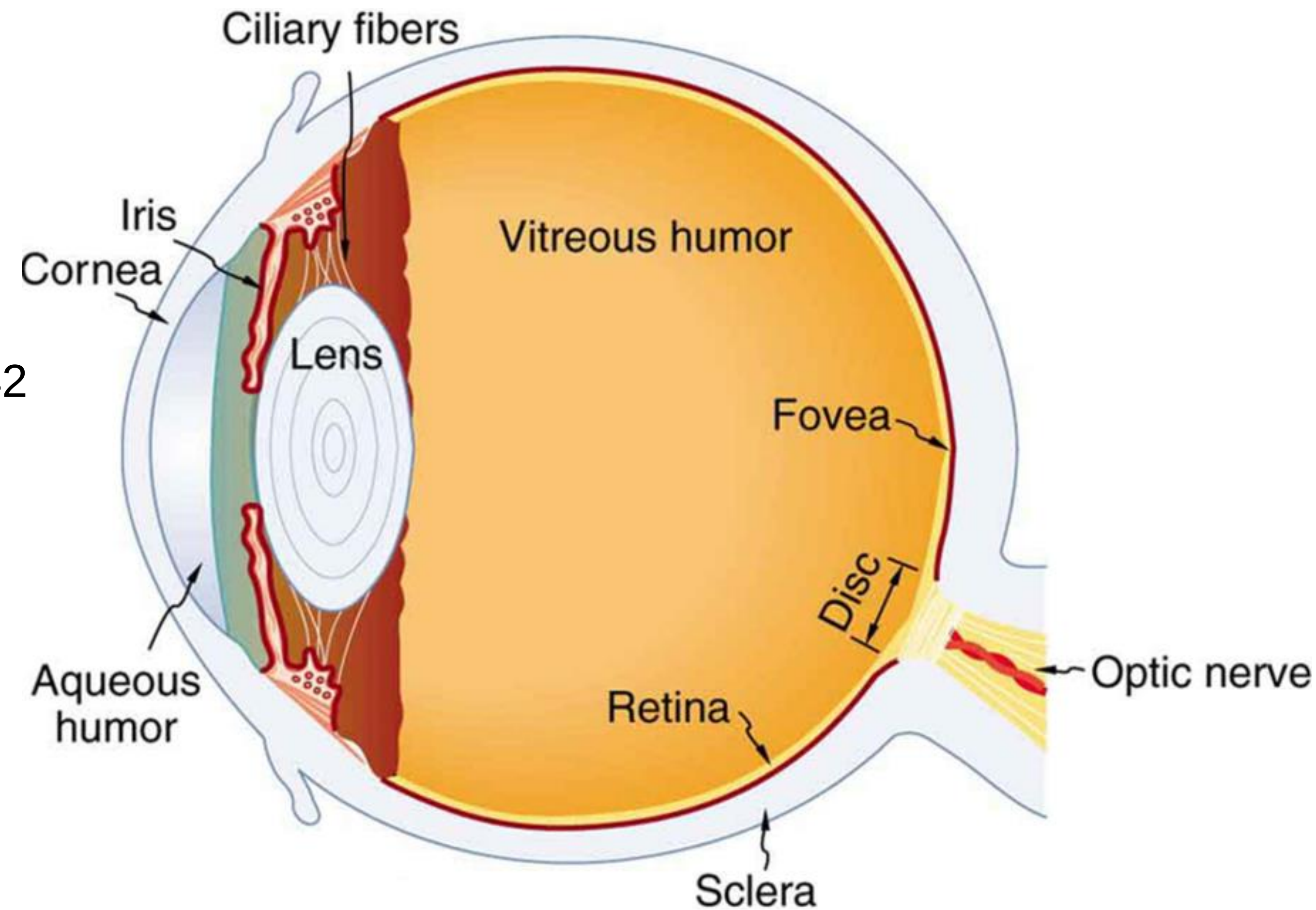

Corneal and ocular aberrations

Null-screen corneal aberrometry

With M. Rodríguez-Rodríguez

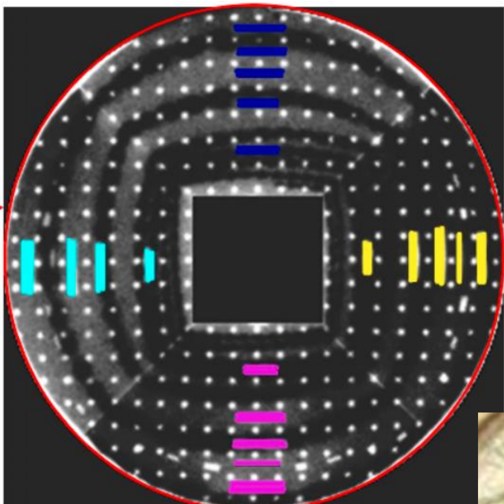

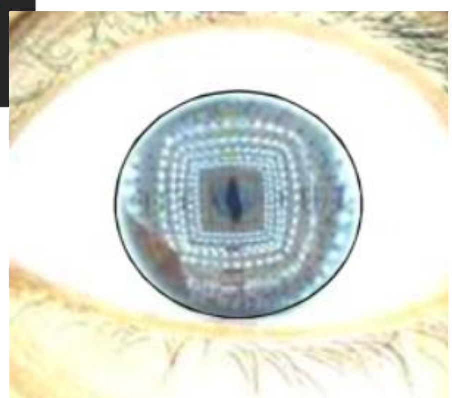

ARVO 2019 + poster MyT2019-123

Manuscript in preparation

Hartmann-Shack ocular wavefront sensing without crosstalk

With A. Carmichael Martins

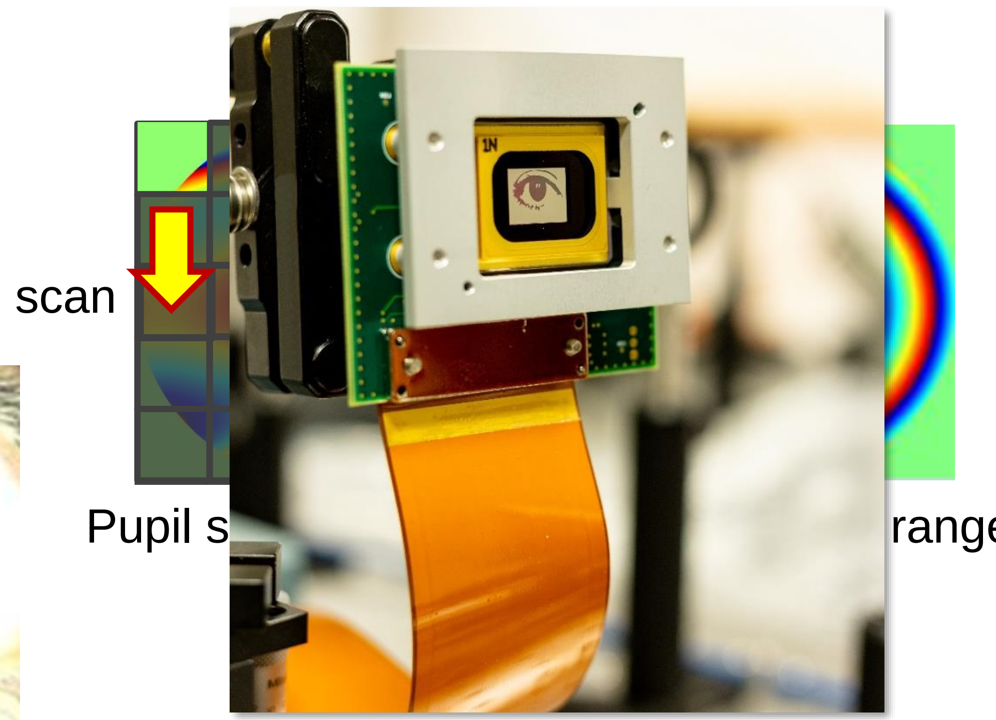

- B. Vohnsen et al., Appl. Opt. 2018
- A. Carmichael and B. Vohnsen, Micromachines 2019

Cones and rods of the human retina

En-face view of parafovea cones and rods

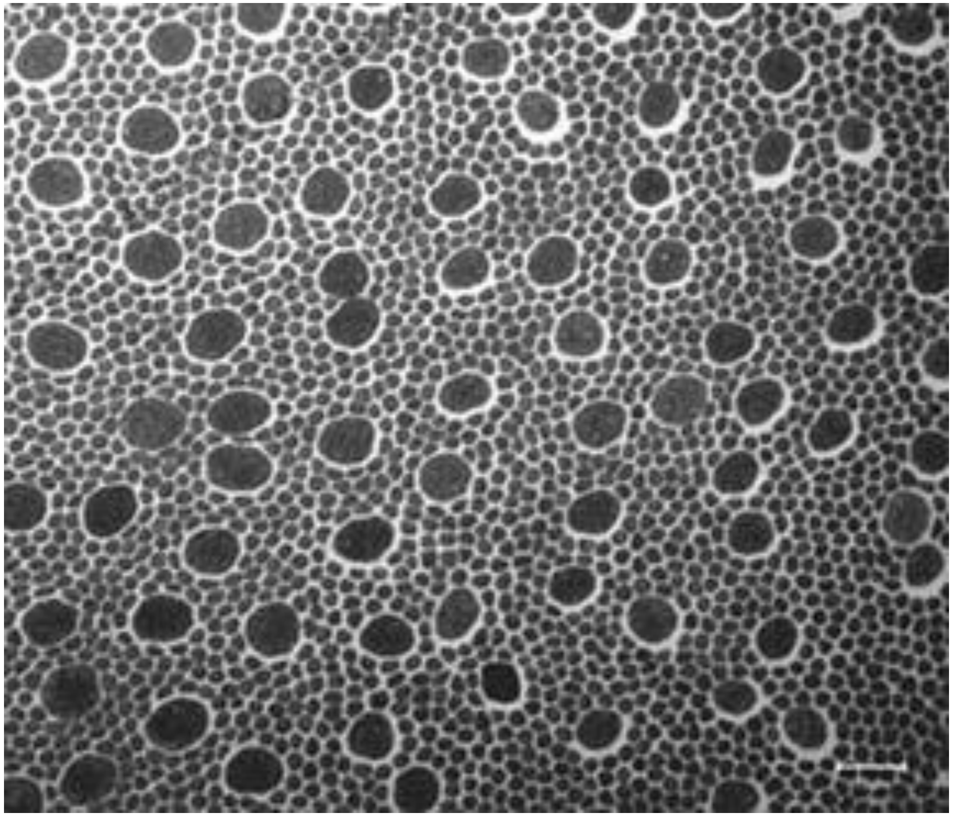

Side view of parafovea cones and rods

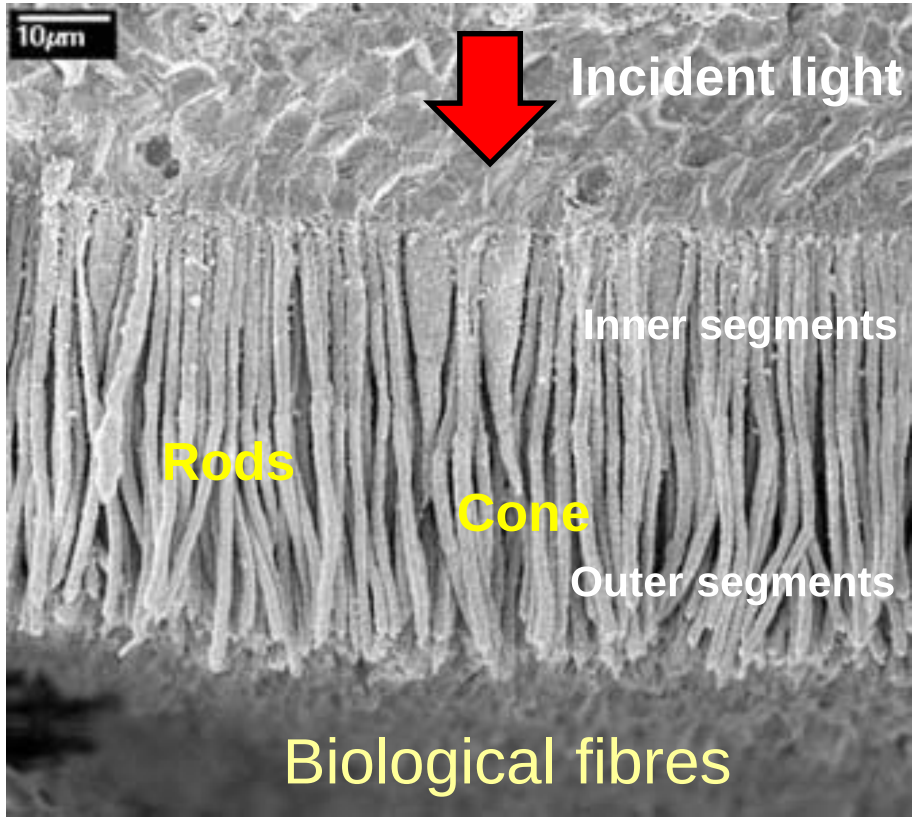

Cone photoreceptor diameter ranging from about 2 μm (fovea) to 8 μm (parafovea)

Images by courtesy of P. Munro, UCL

Eye and retina

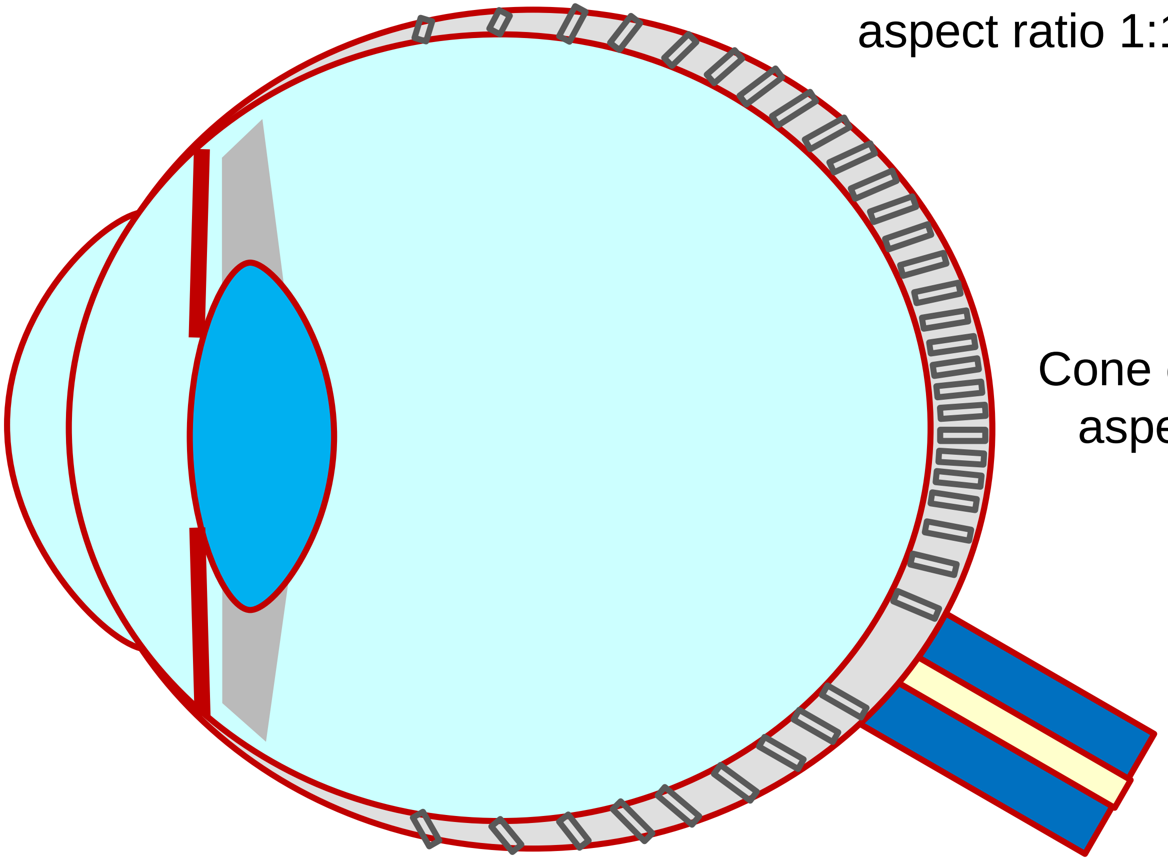

The retina is a tri-dimensional screen

Cones, rods, and ganglion cells

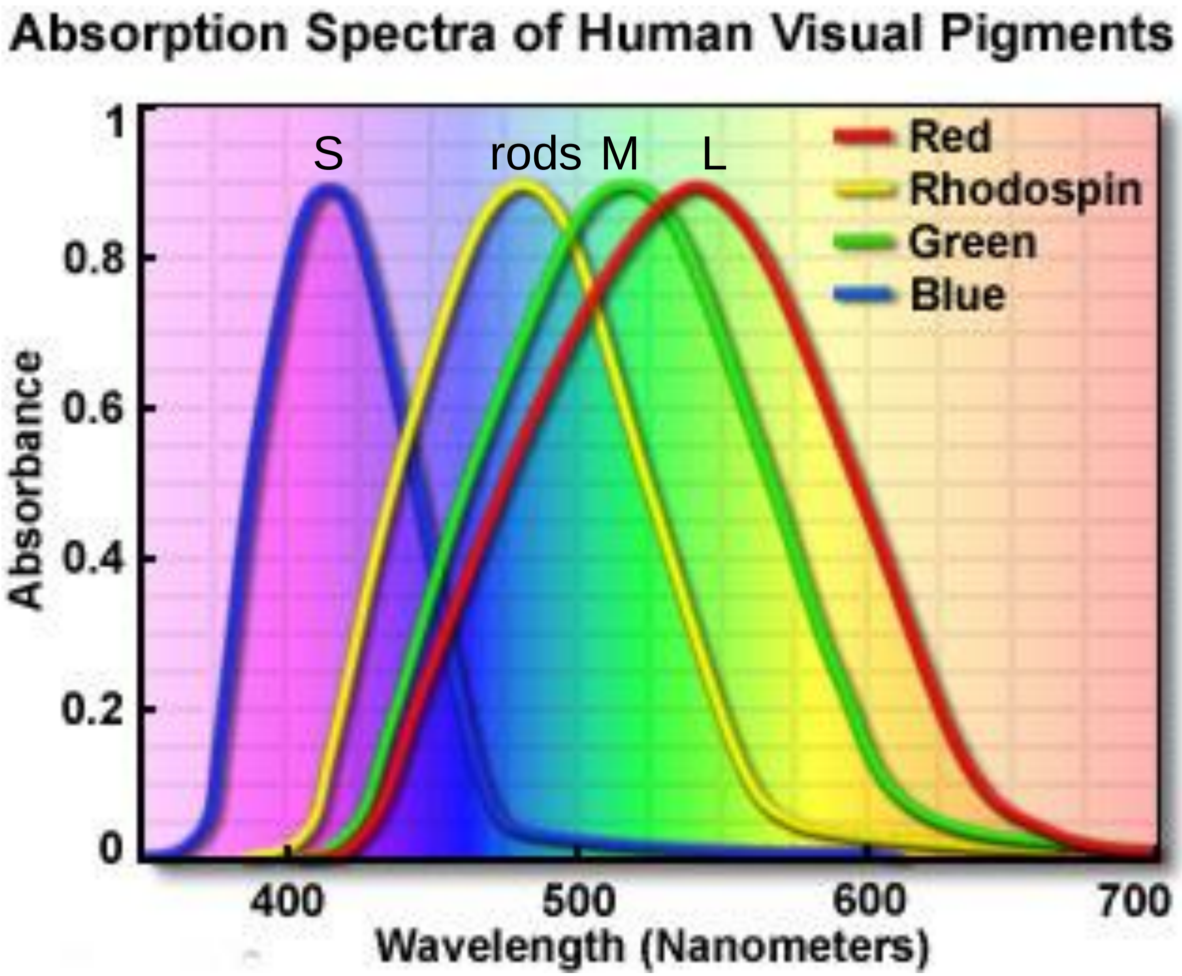

S-cones (420 nm) 5%
M-cones (534 nm) 30%
L-cones (564 nm) 65%
Rods (498 nm)

ipRGC (555 nm)

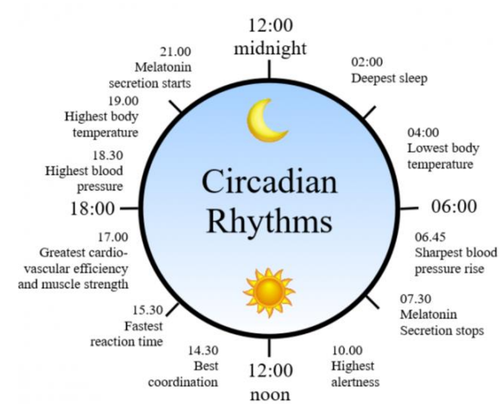

Phototropism in plants

Sunflowers

Photoreceptors are likewise adaptable

Smallman et al., Nature **412** (2001) 604

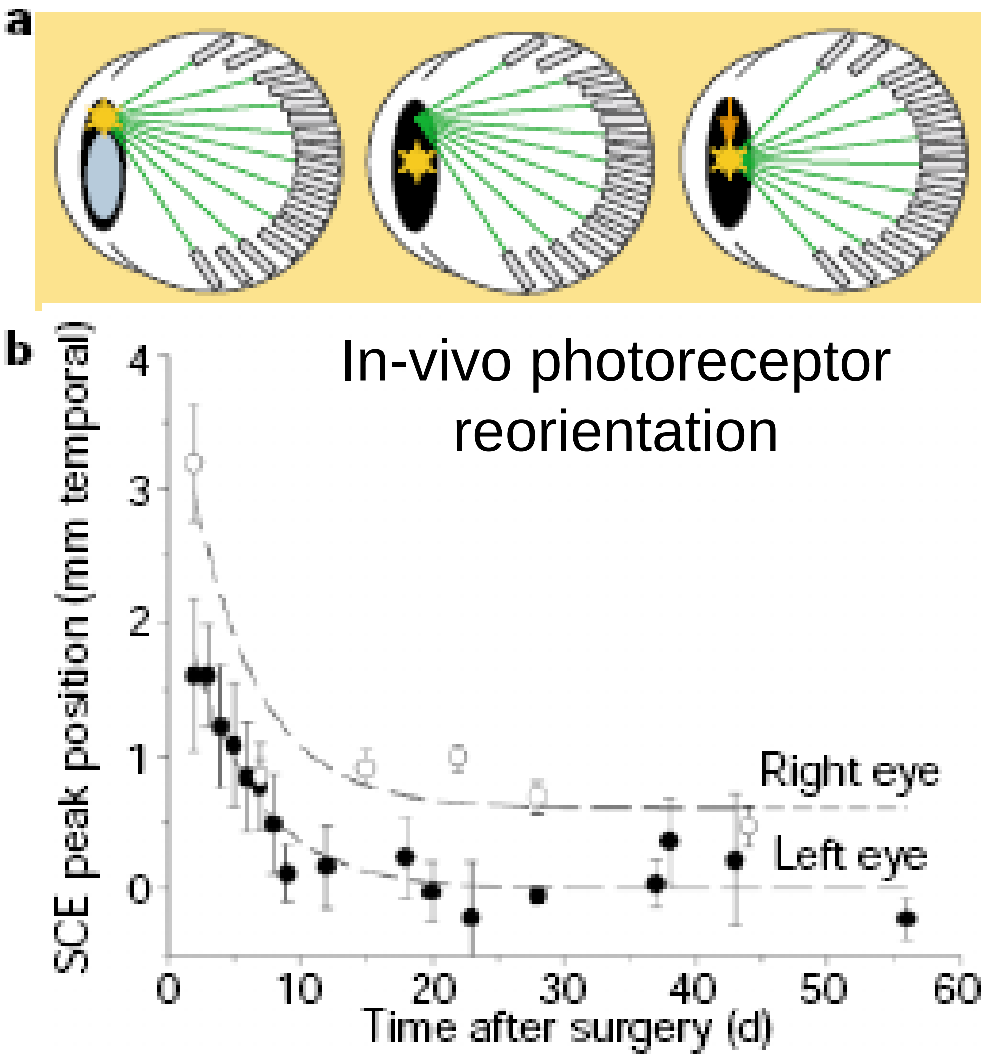

Post-cataract surgery

SCE peak displaced towards new pupil centre

Photoreceptors point to collect a maximum of light (phototropism)

Outline

- The Stiles-Crawford effect(s)
- Photoreceptor waveguides
- Geometrical optics model
- Electromagnetic models
- Myopia, emmetropization, and accommodation
- Directionality in diagnostic imaging
- Conclusions and outlook

Directionality with Maxwellian light

The Stiles-Crawford effect (SCE-I)

Proc. Roy. Soc. 1933

Walter S. Stiles

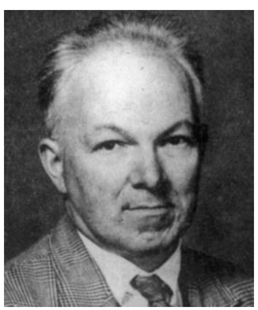

Brian H. Crawford

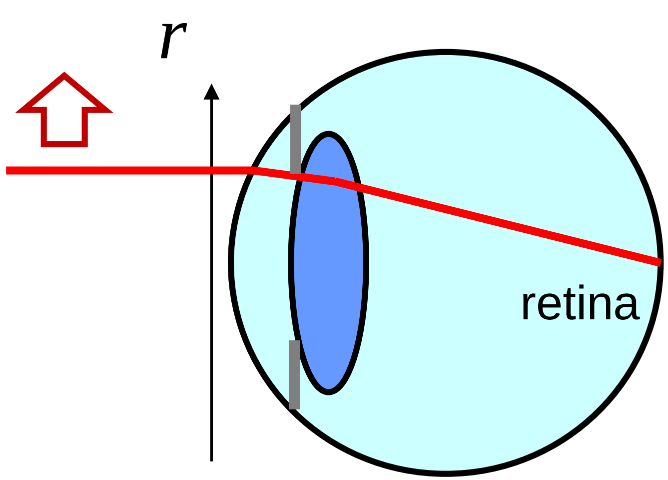

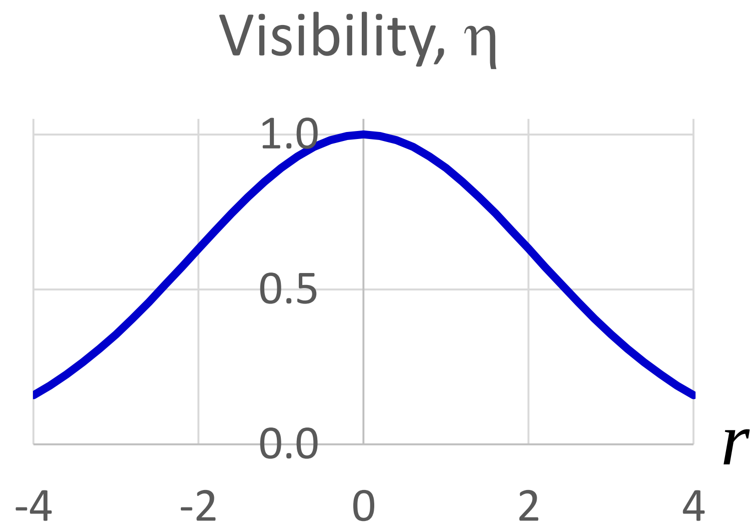

Visibility for oblique rays:

$$\eta(\mathbf{r}) = \eta_{max}(\mathbf{r}_{max})10^{-\rho_{SCE}|\mathbf{r}-\mathbf{r}_{max}|^2}$$

Foveal directionality parameter ⇒ $\rho_{SCE} \cong 0.05/\text{mm}^2$

Maxwellian light

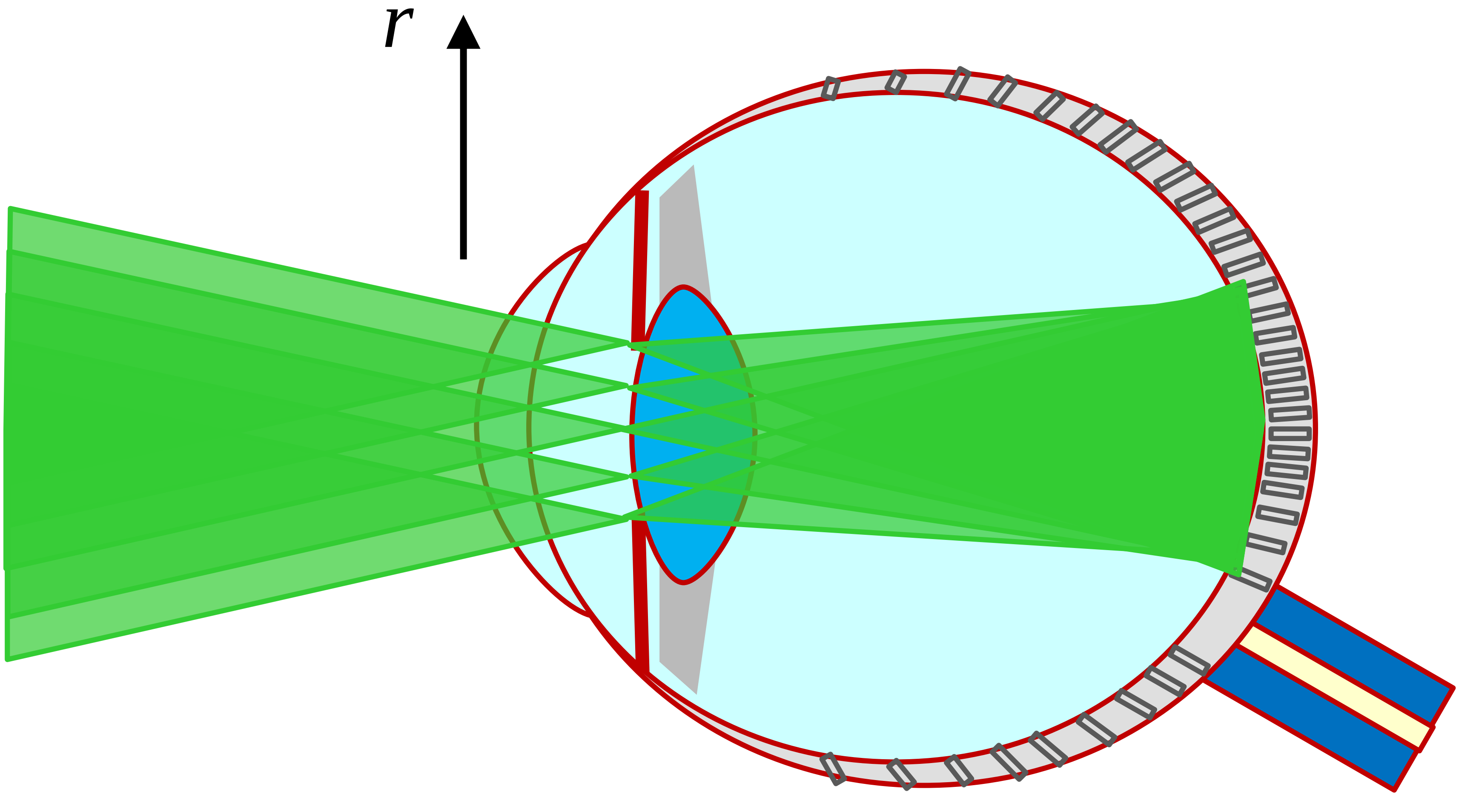

Real-eye cone-photoreceptor waveguides

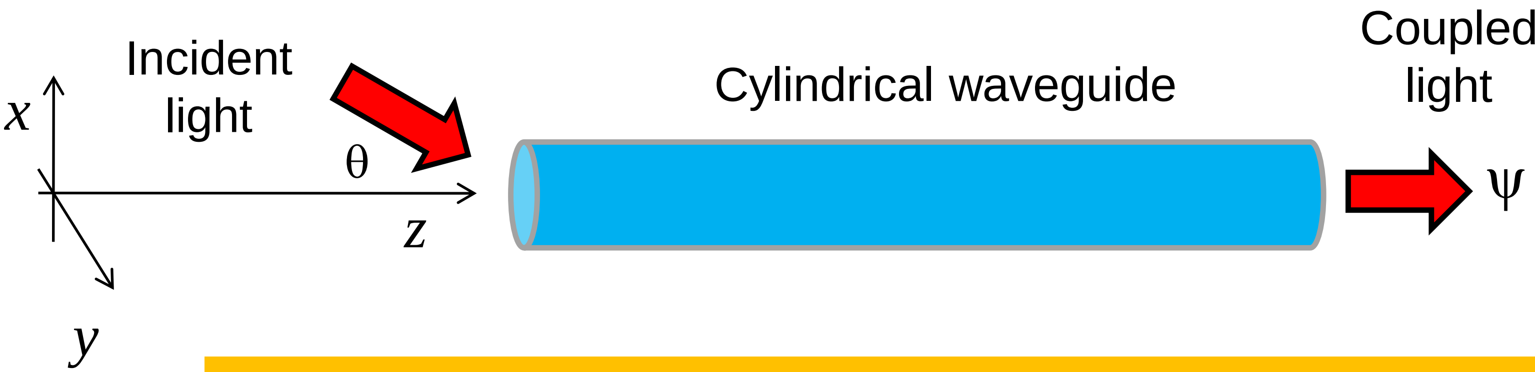

$$\psi = \sum_{n,m} c_{n,m}\, \mathrm{LP}_{n,m}$$

- Fovea cones: single (or few) mode waveguides
- Parafovea cones low-order multimode waveguides

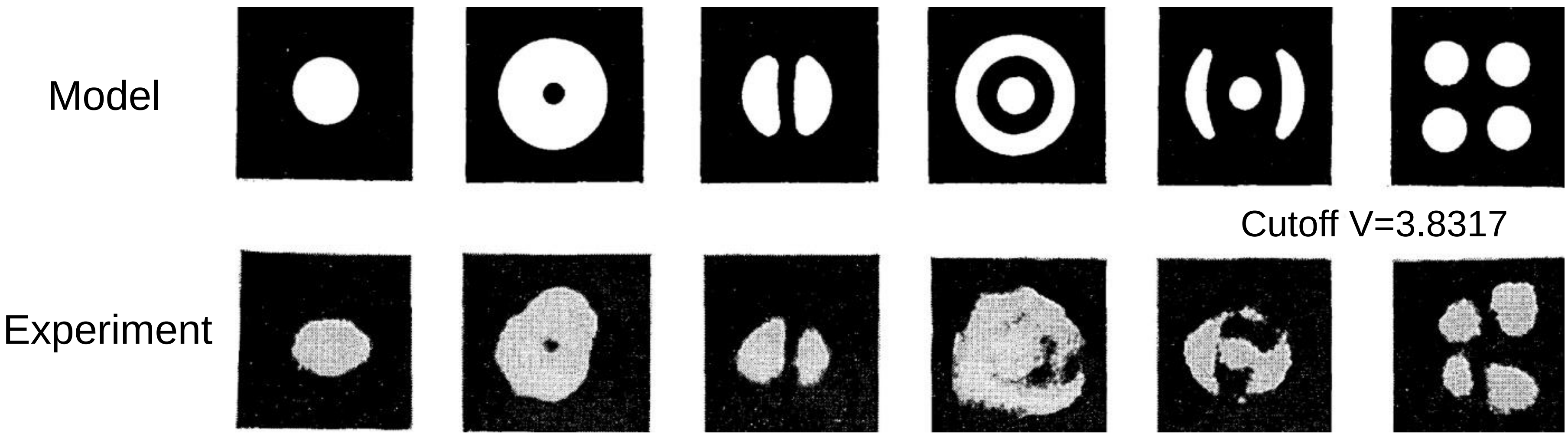

Outer segment modes of **rat, monkey, and human** (Enoch, JOSA 1963)

Mode number

Cylindrical waveguide photoreceptor model

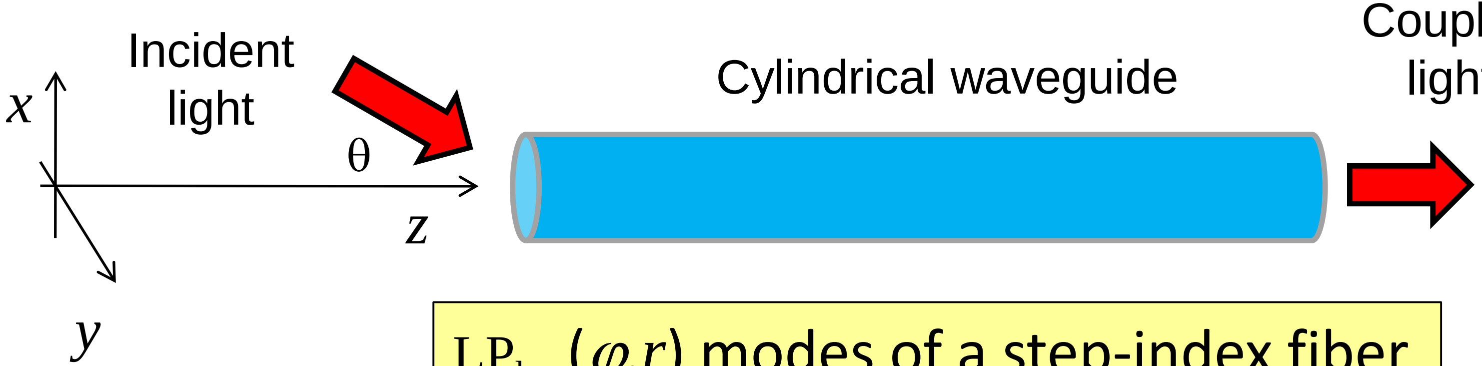

$$\psi = \sum_{n,m} c_{n,m}\, \mathrm{LP}_{n,m}$$

$\mathrm{LP}_{\mathrm{lm}}\,(\varphi, r)$ modes of a step-index fiber

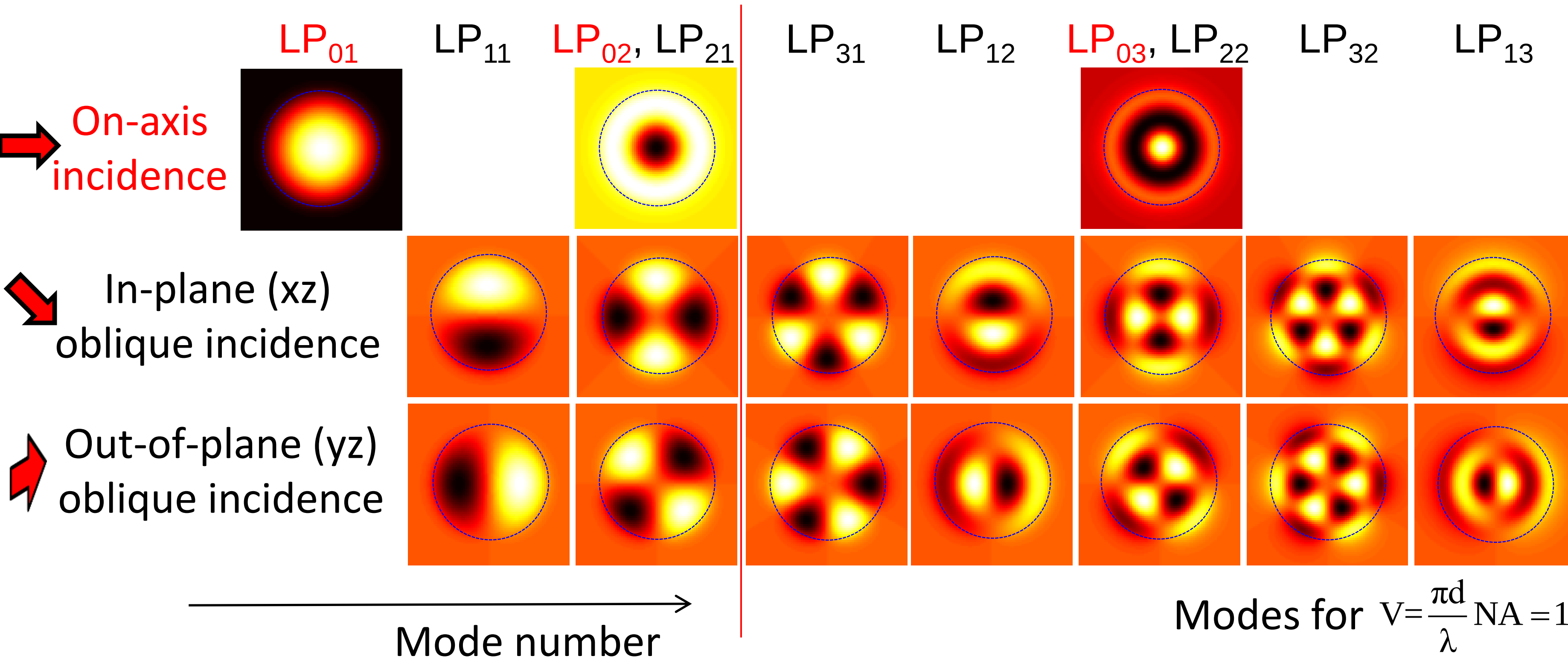

Modes for $V = \frac{\pi d}{\lambda} NA = 10$

Light coupling to a Gaussian mode

Vohnsen *et al*, JOSA A **22** (2005) 2318

Shifting of a narrow incident beam

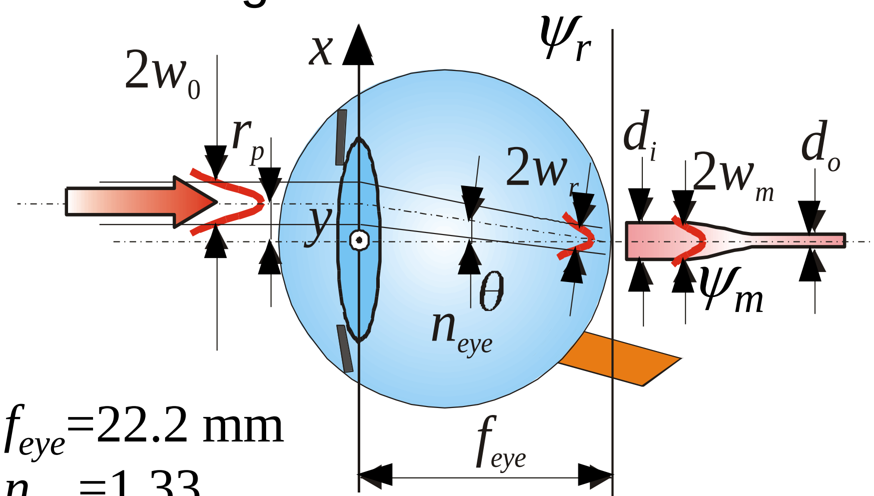

f_{eye}=22.2 mm
n_{eye}=1.33

SCE-I function at the pupil

$$\eta(r) = \eta_{\max} 10^{-\rho_{SCE}(r-r_{\max})^2}$$

Directionality factor

Single waveguide derivation of ρ_{SCE}

Coupling strength:

$$T = \left| \iint \psi_r \psi_m^* du dv \right|^2$$

Gaussian beam and mode approximation (matched $w_m = w_r = w$)

SCE-I directionality factor

$$T(\theta) = \exp\left[-\left(\frac{\pi n_{eye} w}{\lambda} \right)^2 \theta^2 \right]$$

$$\rho_{SCE} = \log(e) \left(\frac{\pi n_{eye} w}{\lambda f_{eye}} \right)^2$$

Normal vision (Newtonian light)

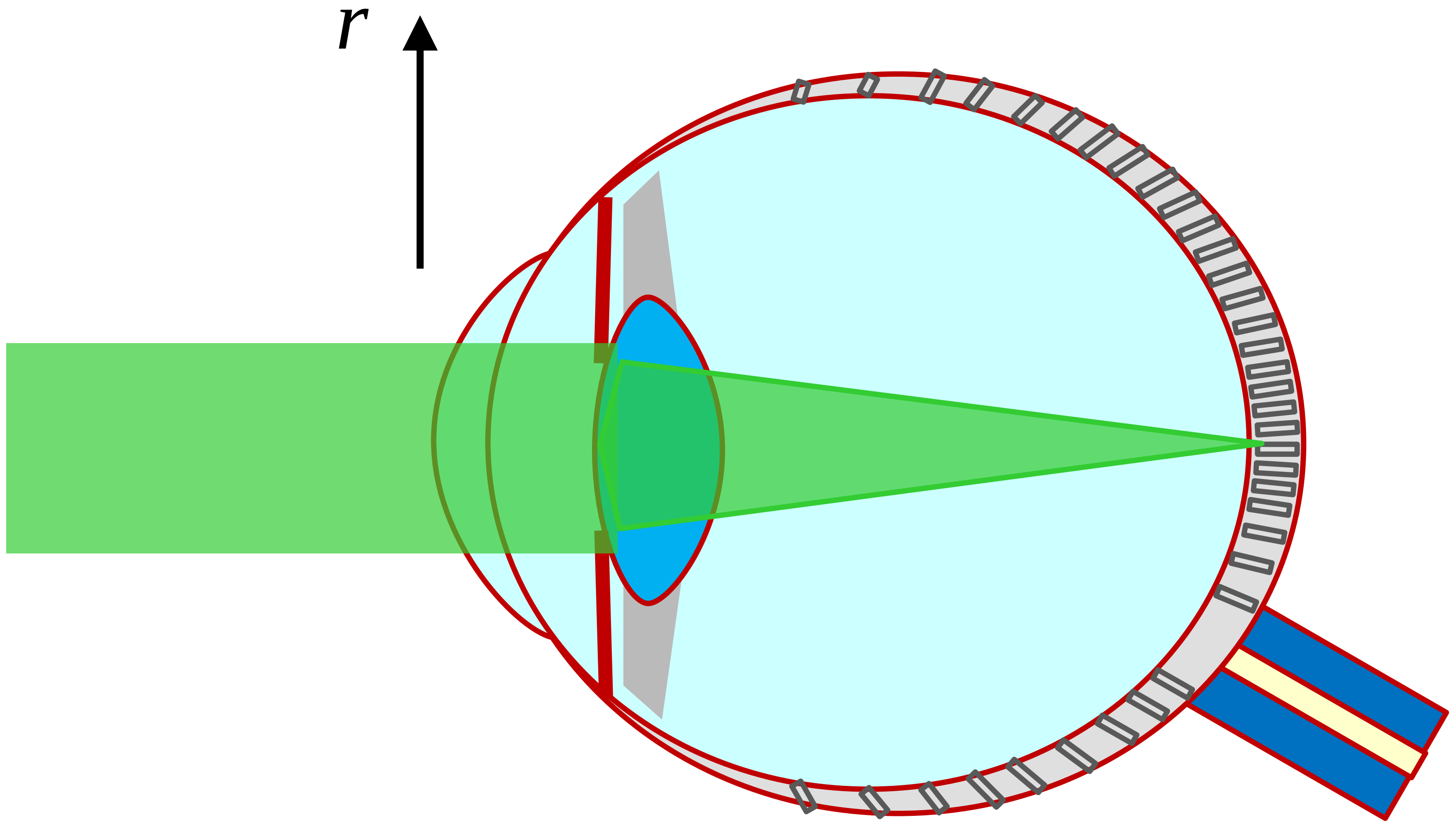

Integrated SCE (normal vision)

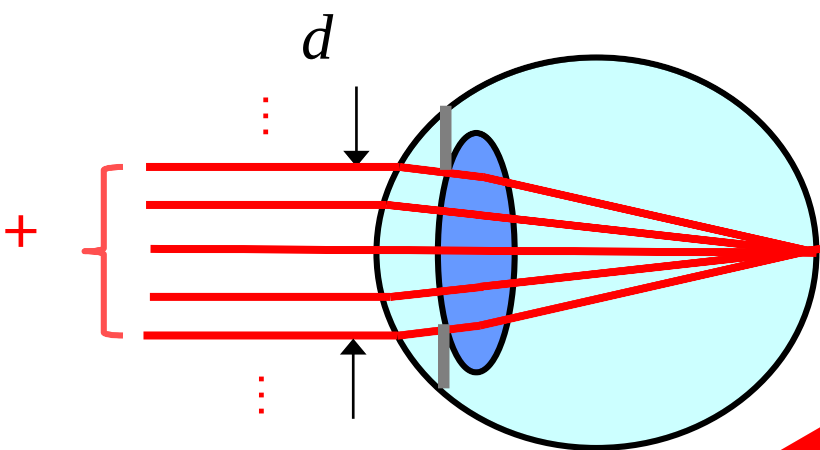

Integrated SCE for a pupil

$\eta_{eff}(d$ … $\rho_{SCE} r^2 \, rdr$ … 0

FALSE

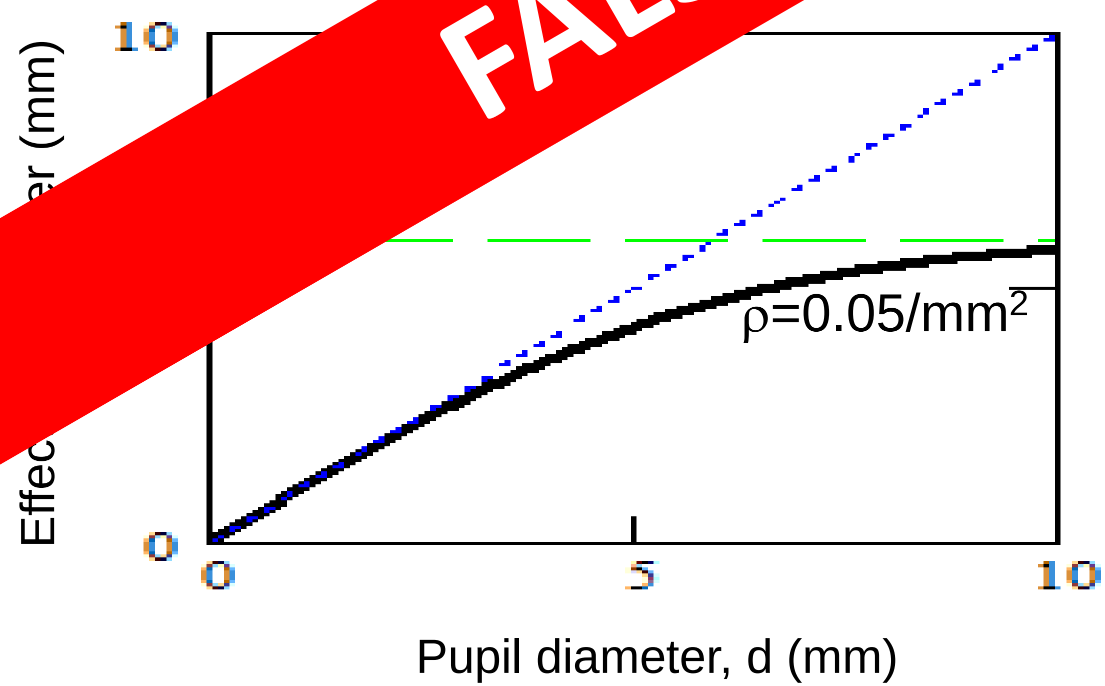

True or false?

What are the Stiles-Crawford effects?

Psychophysical:

SCE-I SCE-II

INTEGRATED SCE-I

Objective:

OSCE

B. Vohnsen, Chapter 18 in Handbook of Visual Optics (Ed. P. Artal, 2017)

What *is* the SCE-I?

Geometrical-optics interpretation

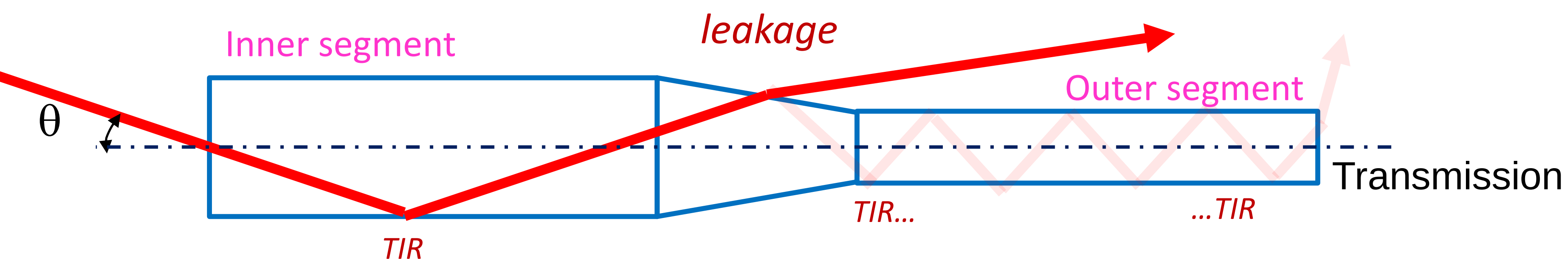

- ❑ Leakage of rays above a critical angle (O'Brien, JOSA 1951)
- ❑ Disarray of neighbouring photoreceptors (Safir & Hyams, JOSA 1969)

Problems?

- ➢ "Sharp" cut-off above a certain angle of incidence
- ➢ This is transmitted light, not absorbed (vision) light
- ➢ How can it describe cylindrical foveal cones? … or rods?

What *is* the SCE-I?

Wave-optics interpretation

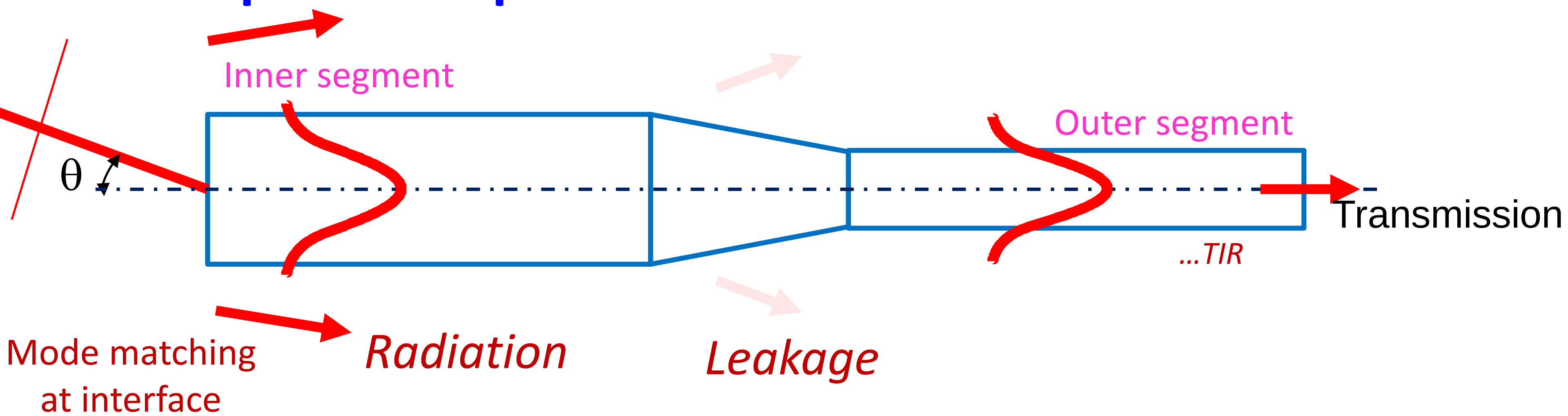

- Fibre-optical waveguide modes (Snyder & Pask, Vis. Res. 1973)
- Gaussian mode coupling (Vohnsen, Iglesias & Artal, JOSA A 2005)

Problems?

- What happens to the nonguided radiative modes?
- This is transmitted light, not absorbed (vision) light
- How can it describe densely-packed waveguides?

Where is vision triggered?

Geometrical-optics solution

We need to consider light *absorption*

Beer-Lambert's law

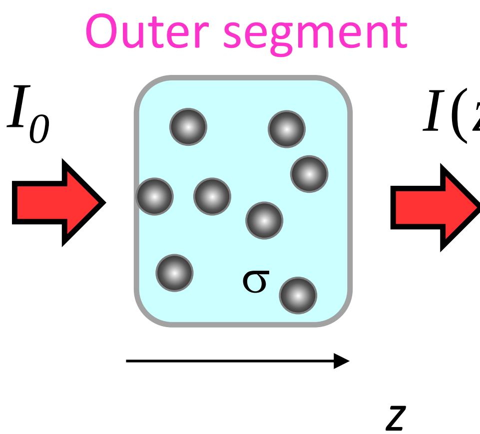

$$I(z) = I_0 \exp(-\alpha z)$$

Visibility (absorption) is proportional to distance (1st order)

$$\eta = 1 - \exp(-\alpha z) \cong \alpha z$$

In 3-D this is a "volumetric" absorption model

Vohnsen et al. J. Vision 2017

Visibility: light-pigment overlap

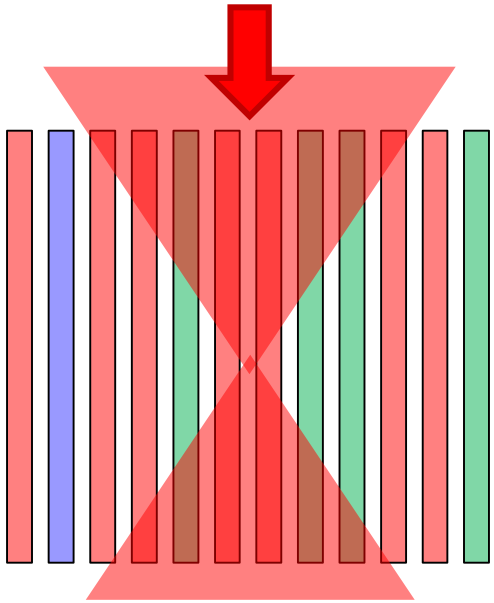

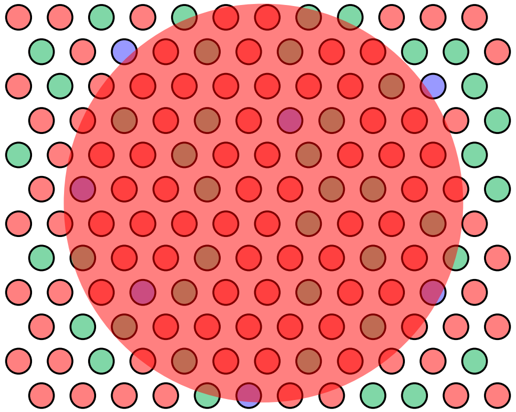

$$\eta = \frac{\text{intersection volume}}{\text{light volume}} \leq 1$$

Volumetric overlap gives an estimate for the absorption and visibility

Example for the SCE-II

Hue shift

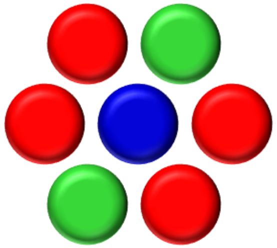

S-cones surrounded by mostly M and L — $\Delta\lambda > 0$

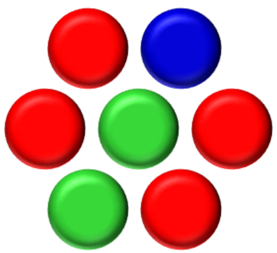

M-cones surrounded by L, M and some S — $\Delta\lambda \cong 0$

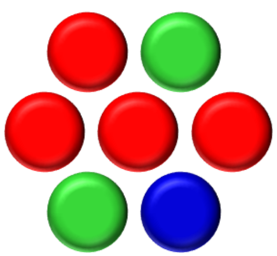

L-cones surrounded by L, M and some S — $\Delta\lambda < 0$

Integrated SCE-I measurements

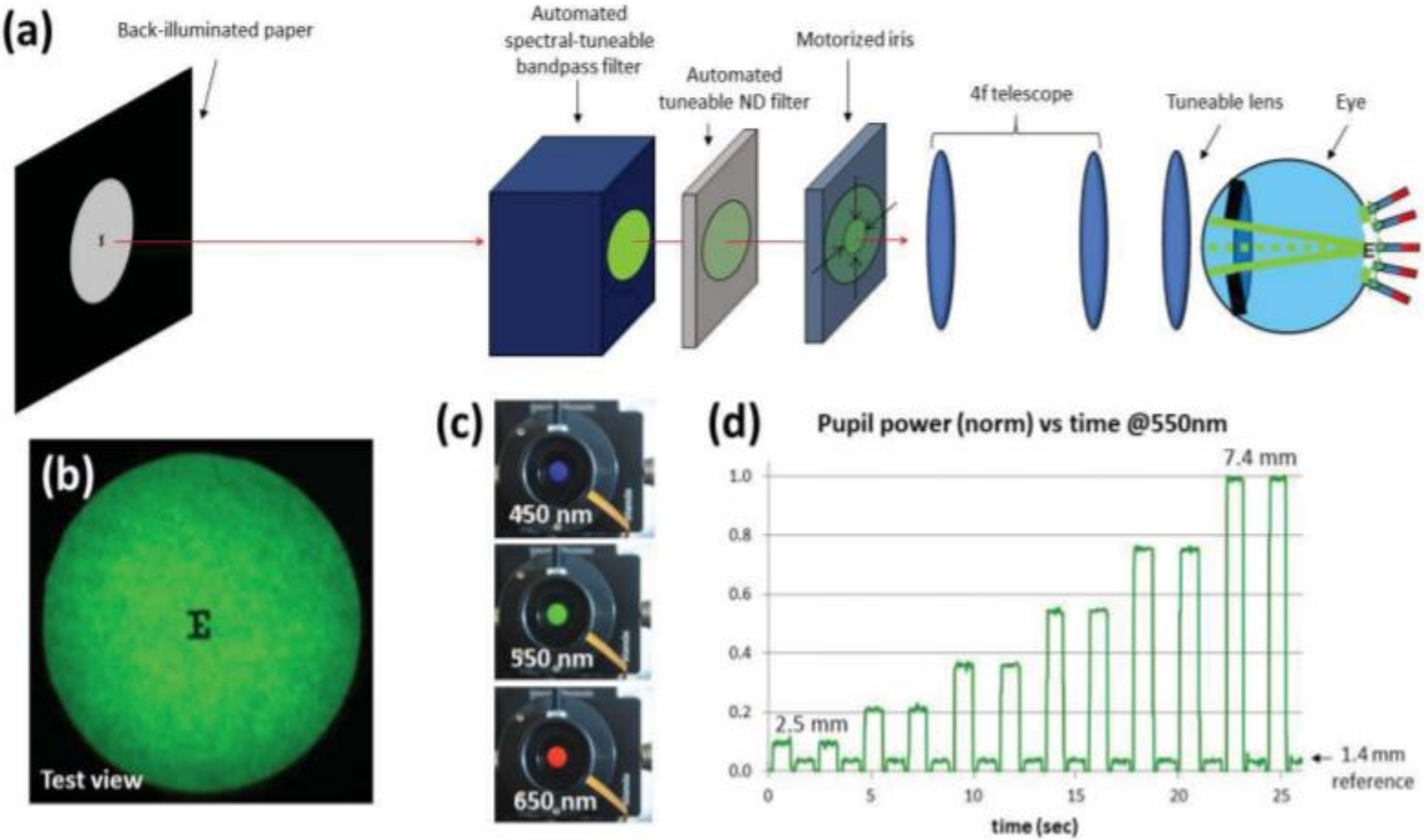

Vohnsen et al. J. Vision 2017

Integrated SCE-I: pupil size flickering

Experimental verification of the volumetric absorption model

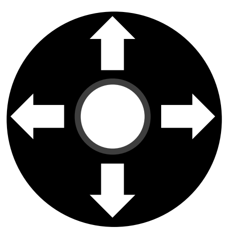

A small pupil is most effective

$\rho \cong 0.40/\text{mm}^2$

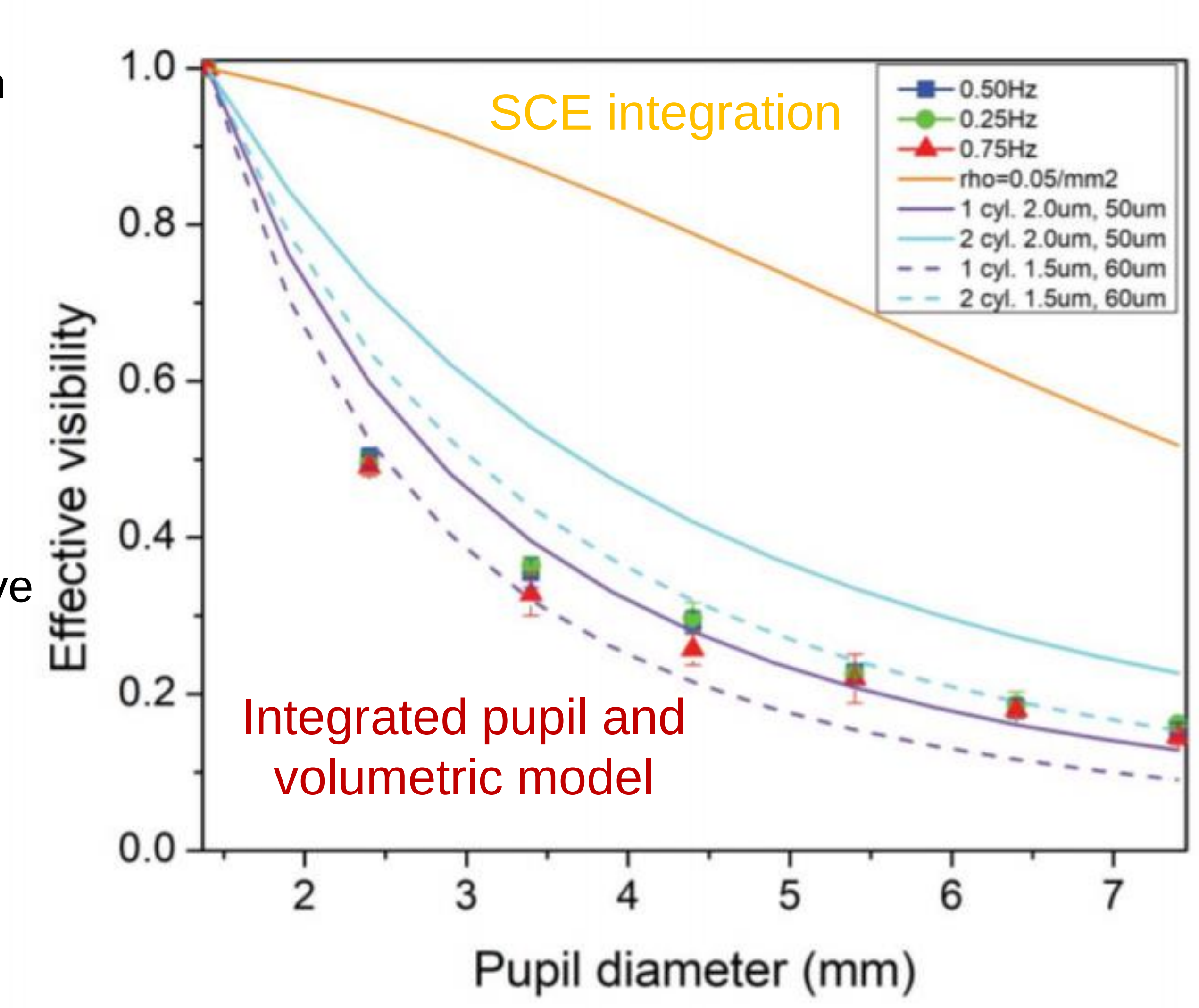

Vohnsen et al. J. Vision 2017

Effective pupil

No SCE-I

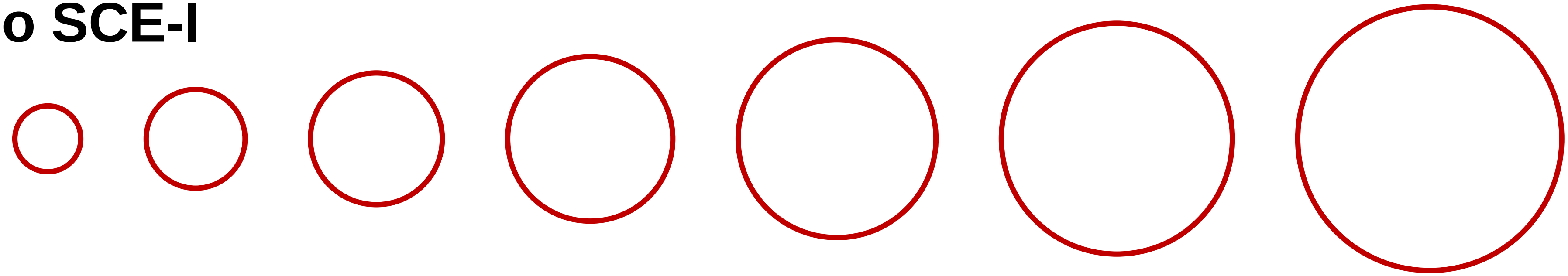

2 mm 3 mm 4 mm 5 mm 6 mm 7 mm 8 mm

ρ = 0.05/mm^2 (Maxwellian light)

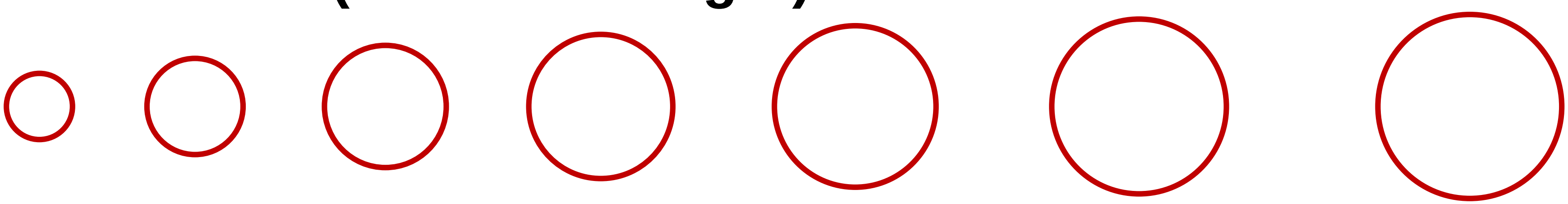

1.94 mm 2.82 mm 3.58 mm 4.22 mm 4.74 mm 5.13 mm 5.41 mm

ρ = 0.40/mm^2 (Normal vision)

1.62 mm 1.95 mm 2.06 mm 2.08 mm 2.08 mm 2.08 mm 2.08 mm

Integrated SCE-I and reduced MTF quality

Vision @ 2 mm pupil

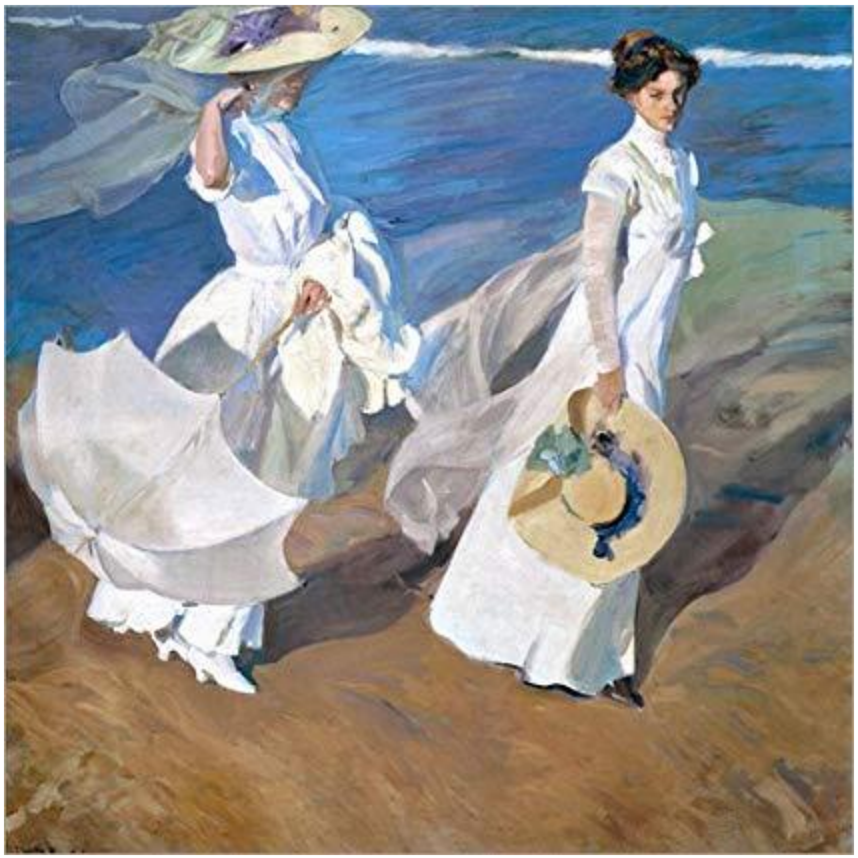

Vision with retinal blur @ 8 mm pupil

Sorolla: walk on the beach (1901)

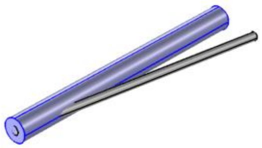

Examples for the SCE-I

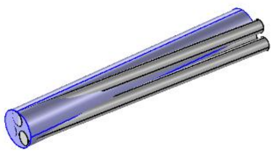

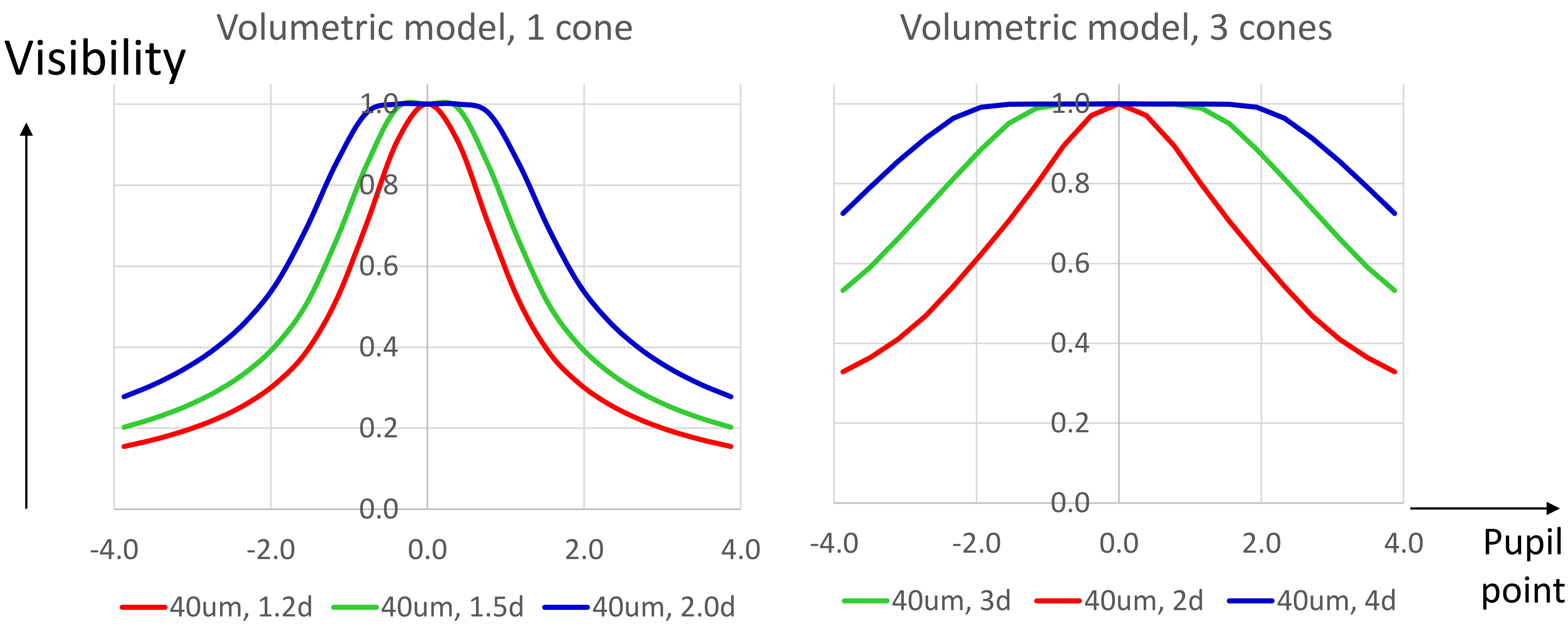

Vohnsen et al. J. Vision 2017

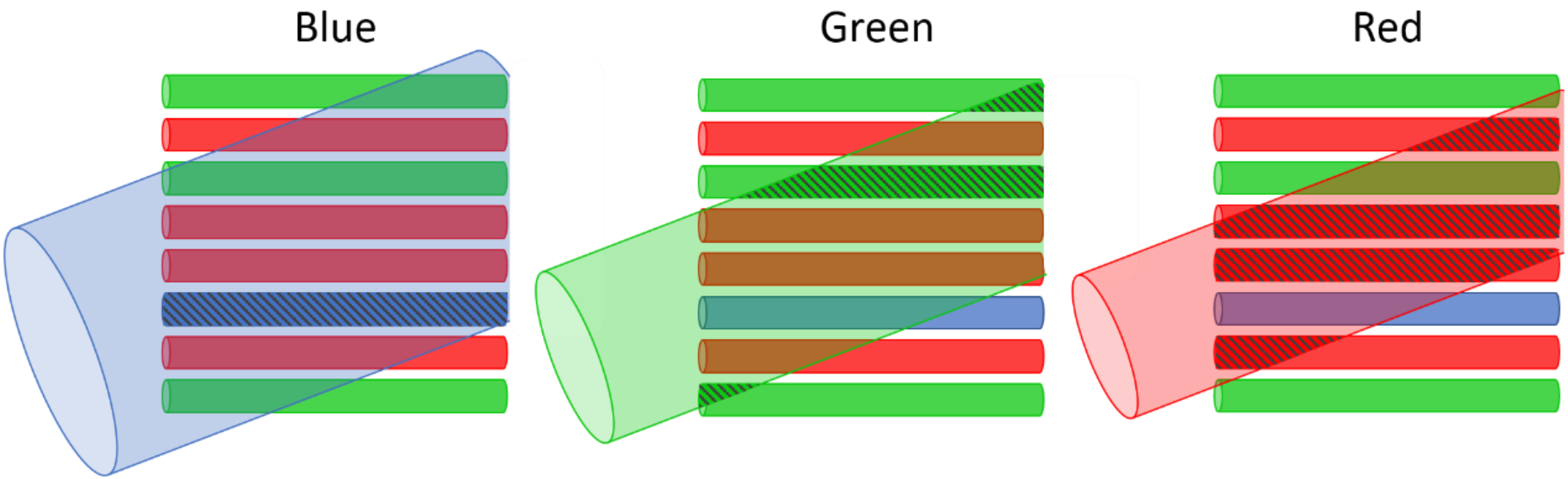

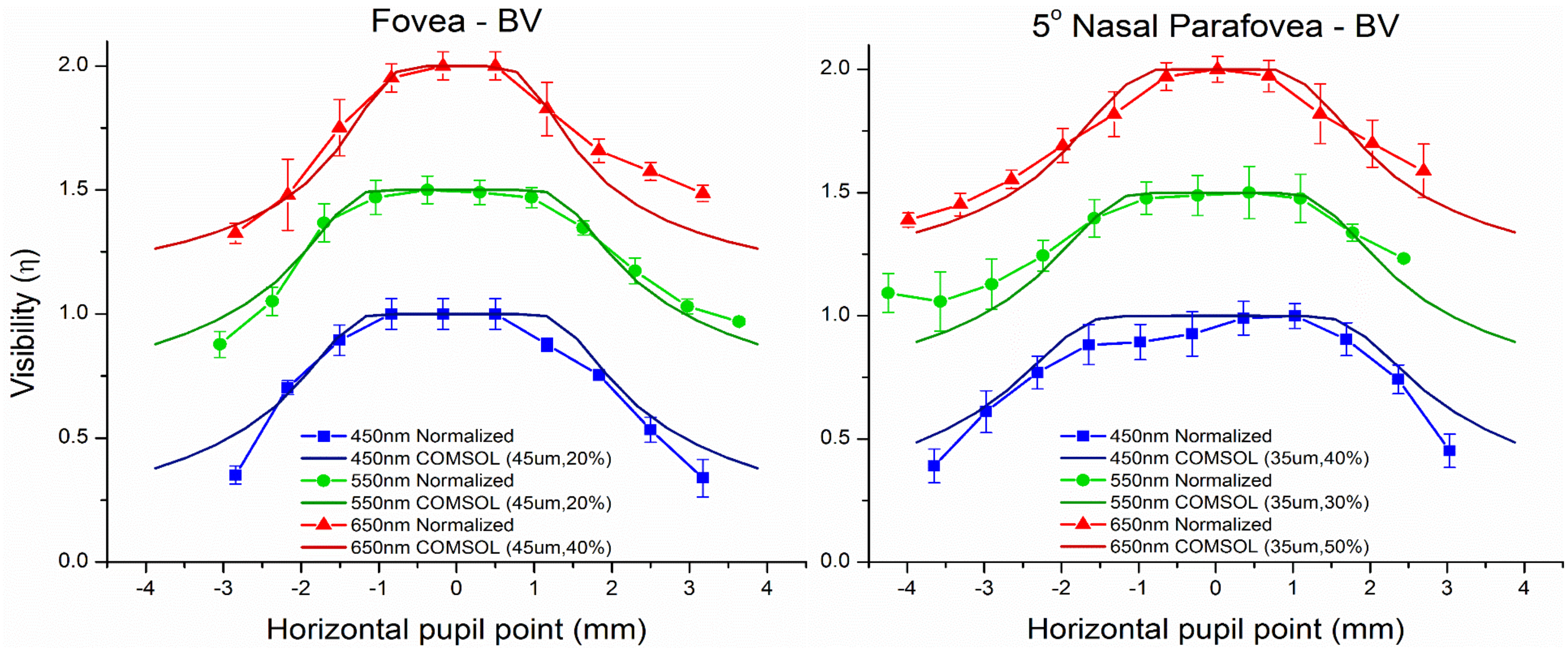

A. Carmichael Martins and B. Vohnsen, Biomed. Opt. Express (submitted, 2019)

Why do rods lack directionality?

Rods are surrounded by … rods

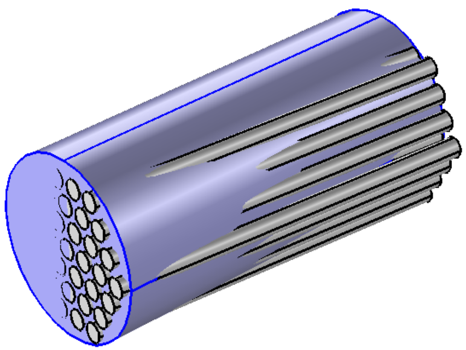

$\Rightarrow \quad \rho_{SCE} \cong 0$

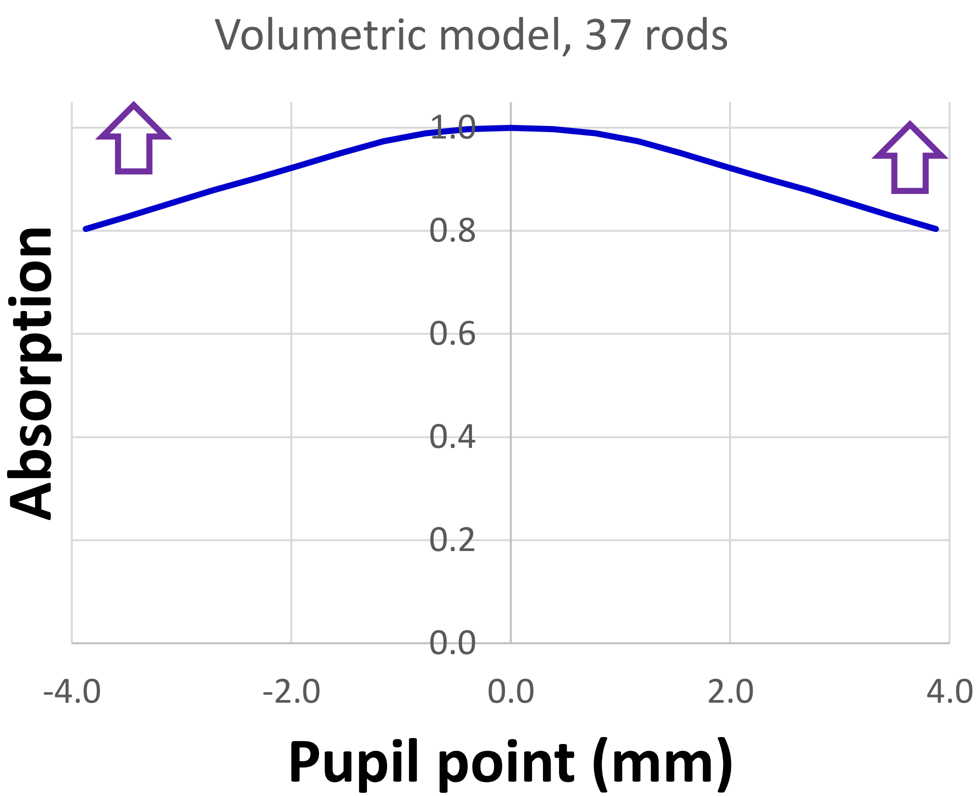

Vohnsen et al. J. Vision 2017

Antenna model

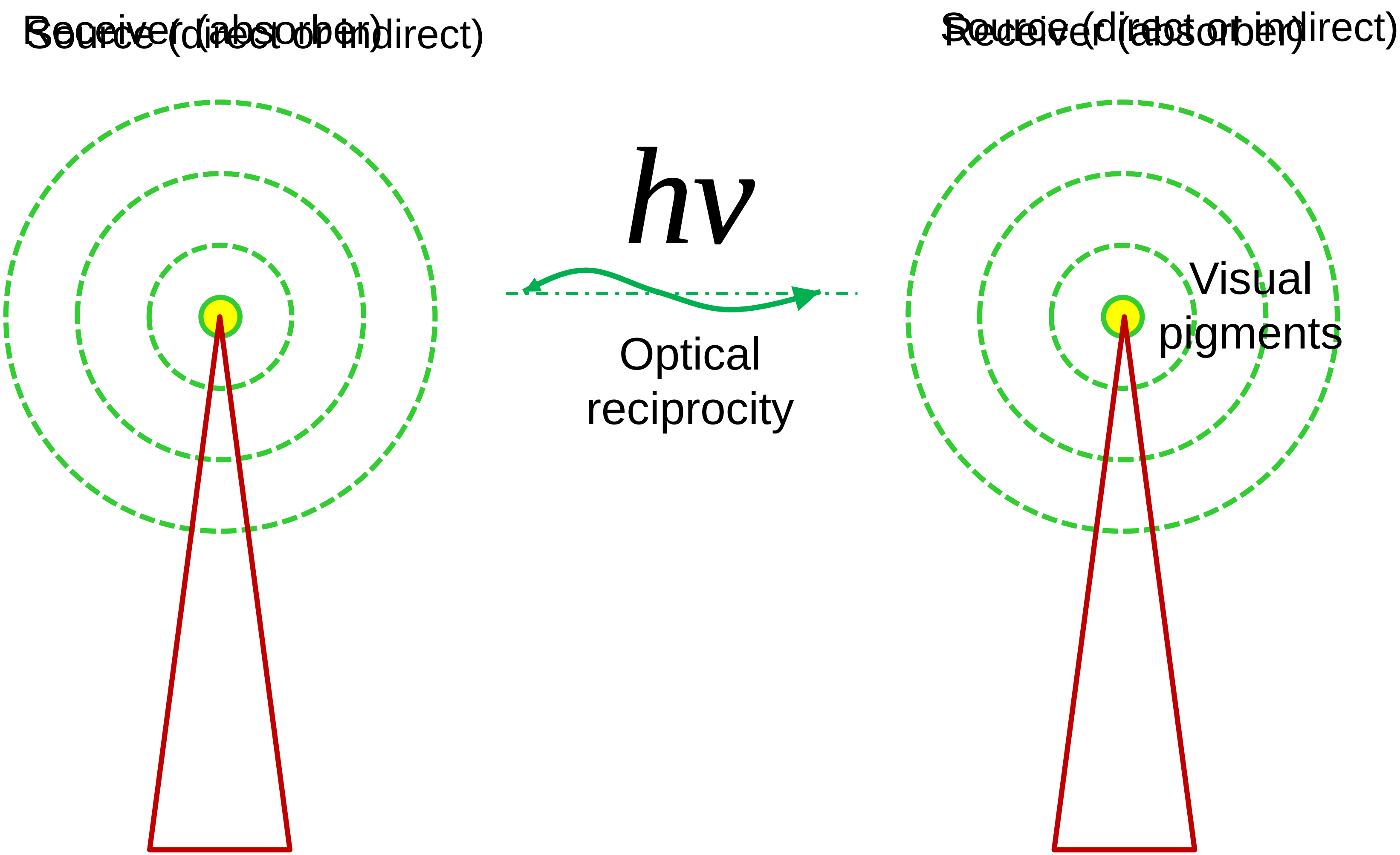

Vohnsen, Biomed. Opt. Express 2014

Outer segment membrane stacking and visual pigments

Modelo de tortillas

Dipolar antenna model of outer-segment pigments

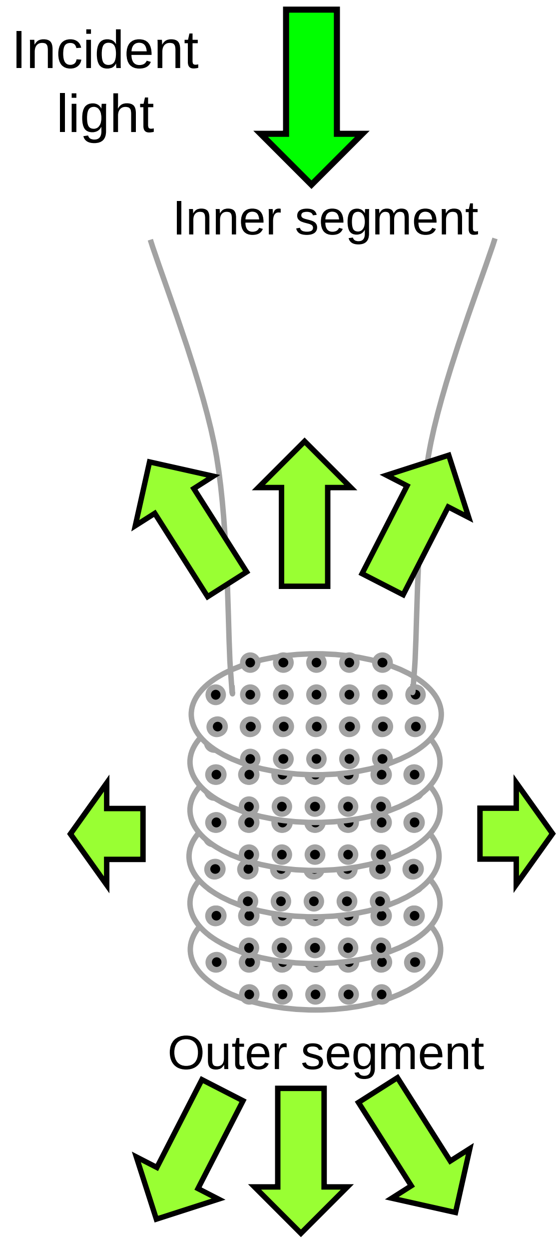

Model data:

Pigments can be considered as dipole antennas (∅5 nm)

Each disc has from 4,000 (∅1 µm) to 4,000,000 (∅5 µm)*

Each outer segment has approximately 1000 lamellae*

Lamellae interspacing is approximately 20 nm*

Membrane wall thickness (5 nm) is ignored

Dipoles are assumed to be uncoupled

*J. J. Wolken, "Light detectors, photoreceptors, and imaging systems in nature" (Oxford, 1995)

Diffraction equivalence (1 disc)

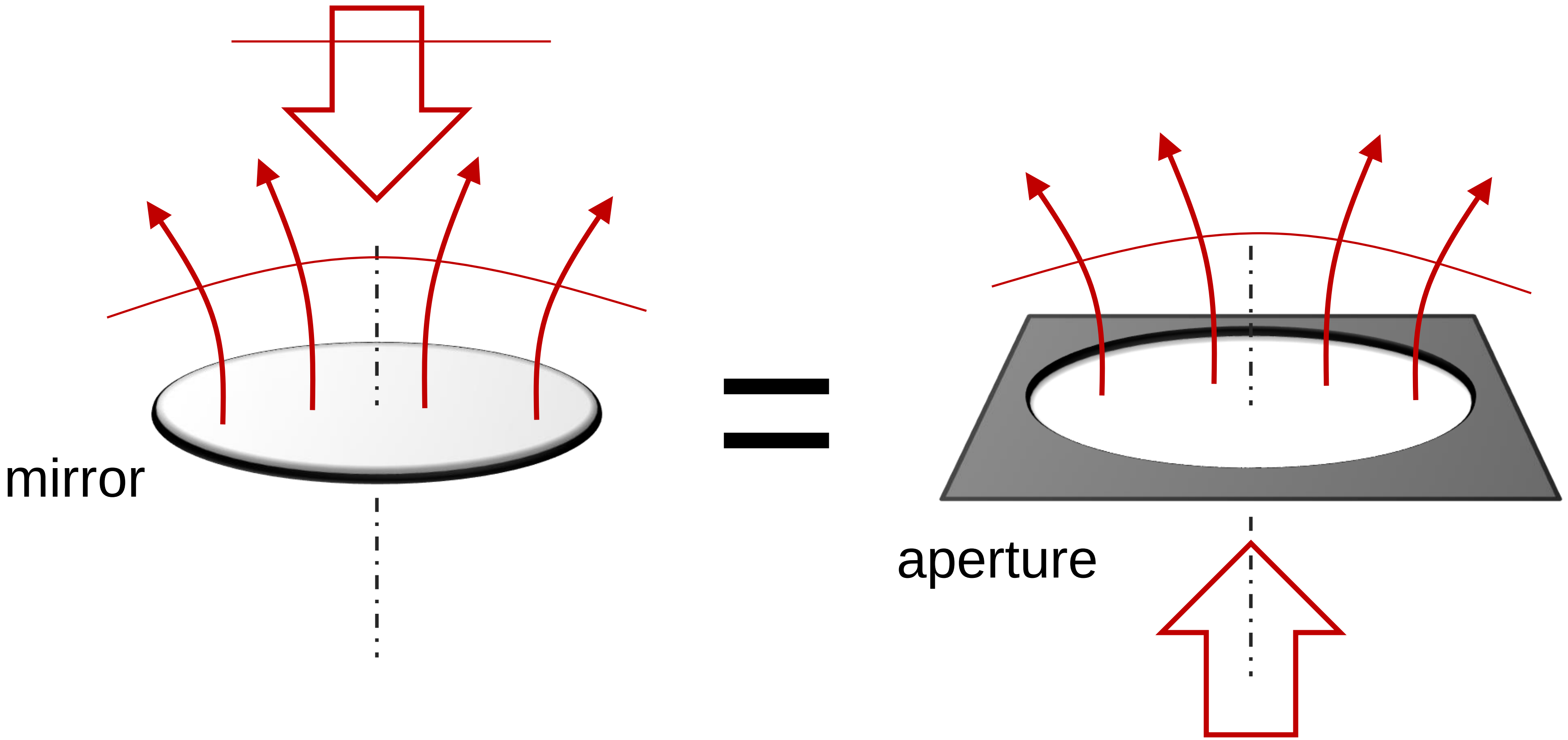

B. Vohnsen, The retina and the Stiles-Crawford effects, in Handbook of Visual Optics 2017, Ch. 18

Electromagnetic *scattering* model

Multilayer antenna model and optical reciprocity

$\Rightarrow$ ρ in the range of 0.05 (dim light) – 0.10 /mm^2 (bleached)

Outer segment membranes or equivalently stacked apertures

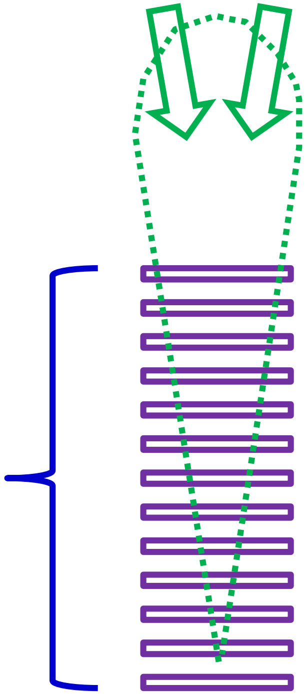

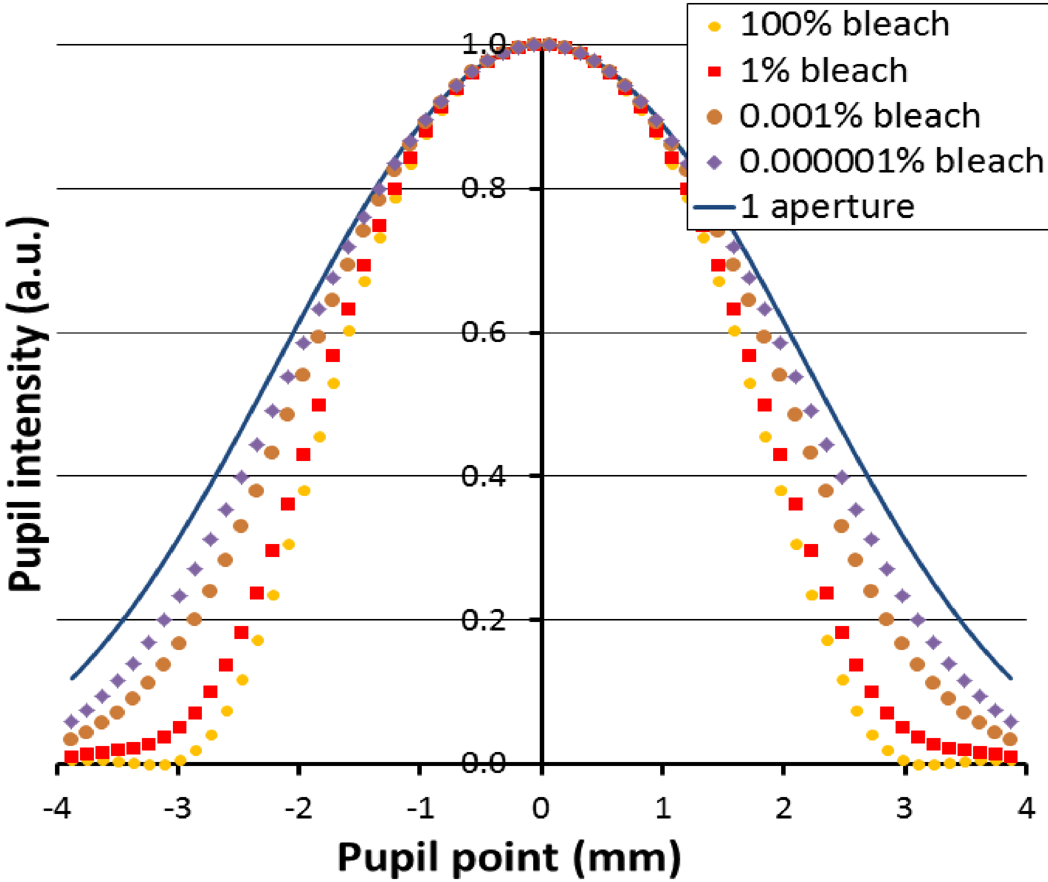

Vohnsen, Biomed. Opt. Express 2014

Oblique incidence on one outer segment

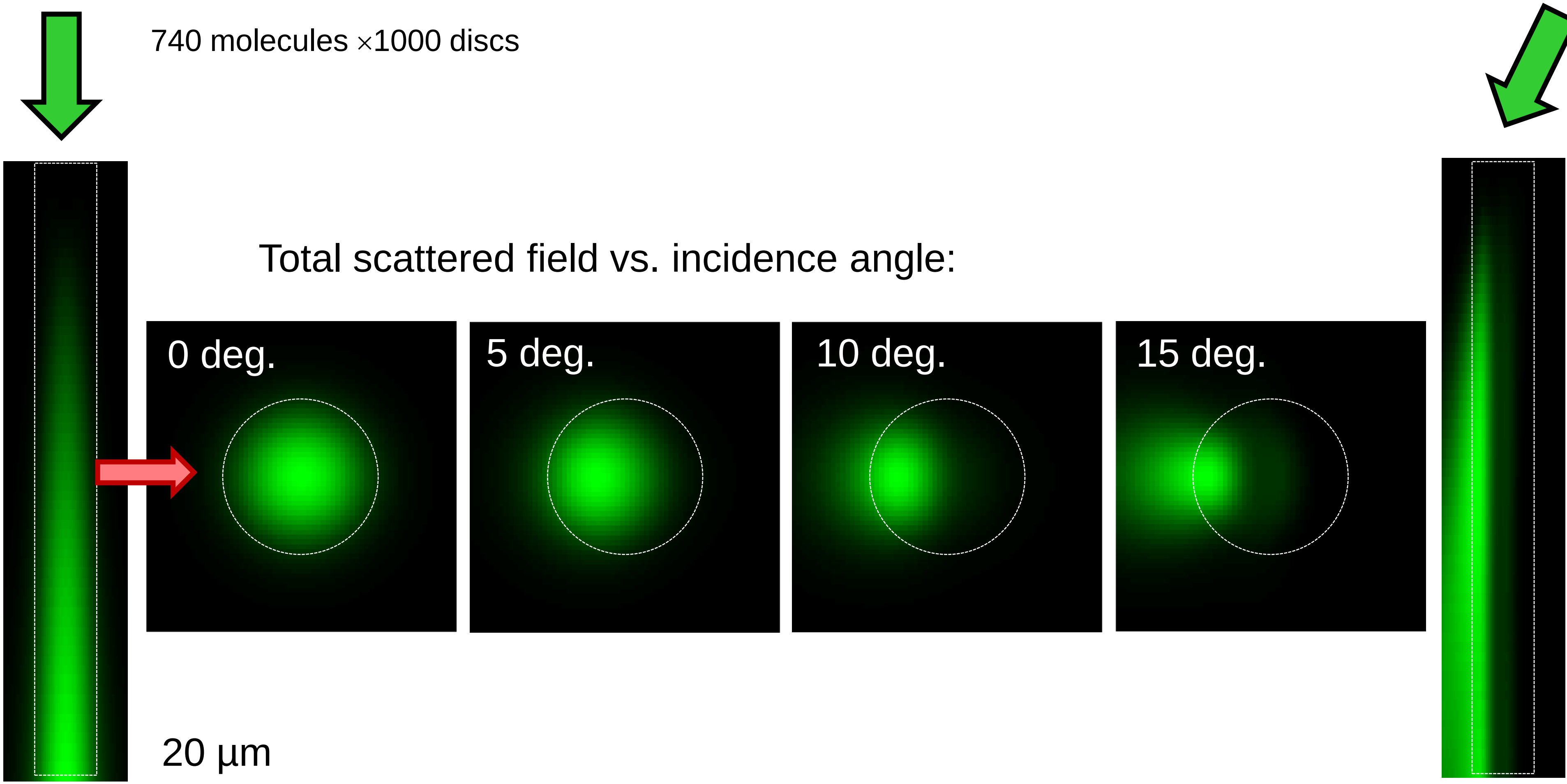

For oblique incidence, scattered light shifts to one side of the segment.
With a conical outer segment (not shown) the axial light becomes more confined

A "new" Stiles-Crawford fitting function

Airy-disc pupil function for relative visibility/intensity:

$$\eta(\boldsymbol{r}) = \eta_{\max}(\boldsymbol{r}_{\max})\left[2\frac{J_1(\alpha|r-r_0|)}{\alpha|r-r_0|}\right]^2$$

Peak of visibility (or intensity)

New directionality parameter

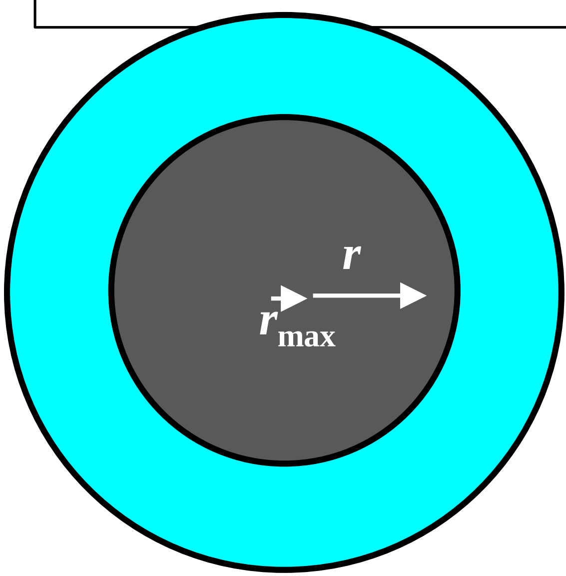

Vohnsen, Biomed. Opt. Express 2014

Gaussian vs. Airy SCE-I function

Subject BV 550nm (experiment)
12 measurement-series averaged

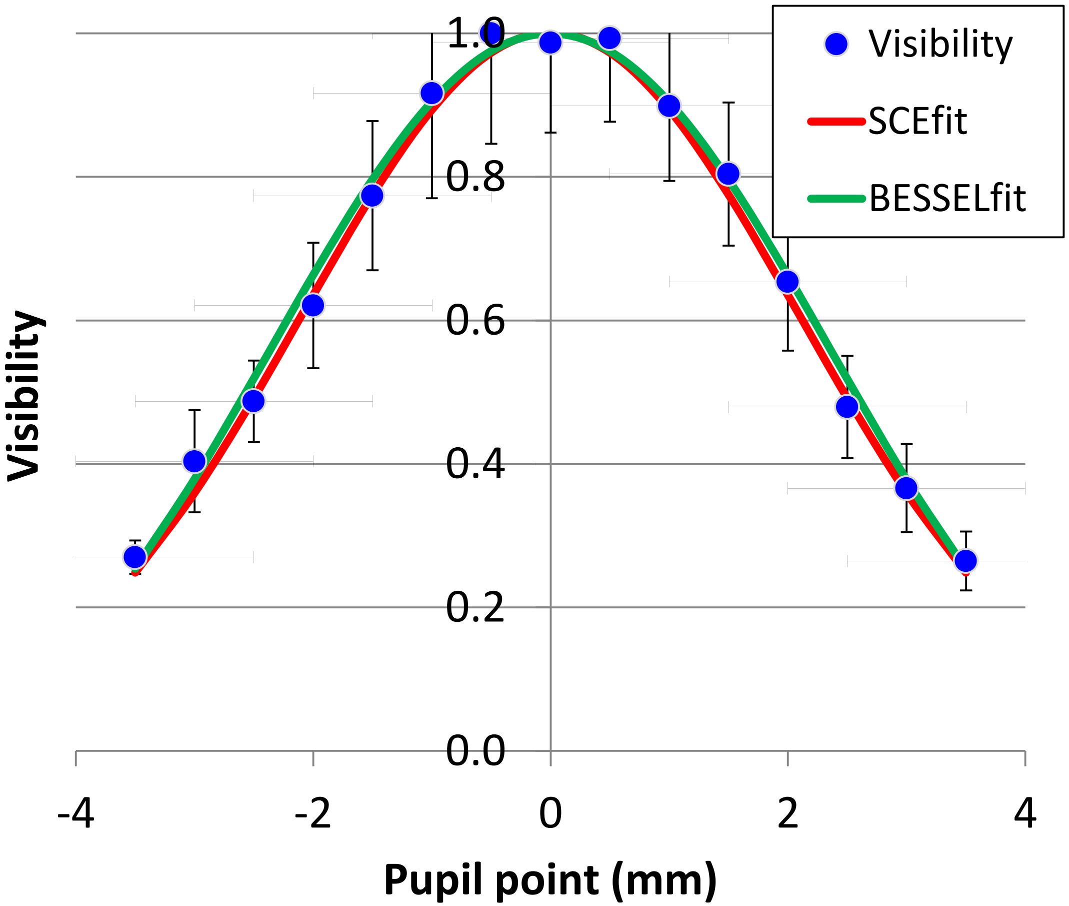

Gaussian SCE function?

$$\eta(r) = 10^{-\rho(r-r_0)^2}$$

or Airy disc function?

$$\eta(r) = \left[2\frac{J_1(\alpha(r-r_0))}{\alpha(r-r_0)} \right]^2$$

B. Vohnsen, The retina and the Stiles-Crawford effects, in Handbook of Visual Optics 2017, Ch. 18

Increased myopia prevalence

Excessive eye growth affecting 50% of the world population by 2050

Increased risk of retinal detachment and glaucoma

“The myopia boom” Nature (2015)

SCE-I analysed in myopes, uniaxial system

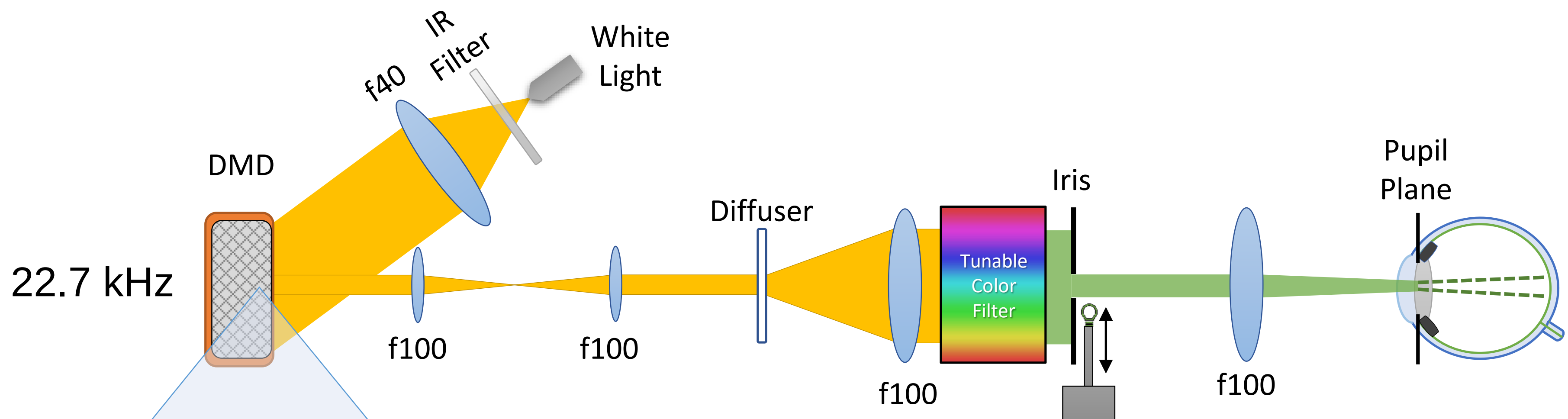

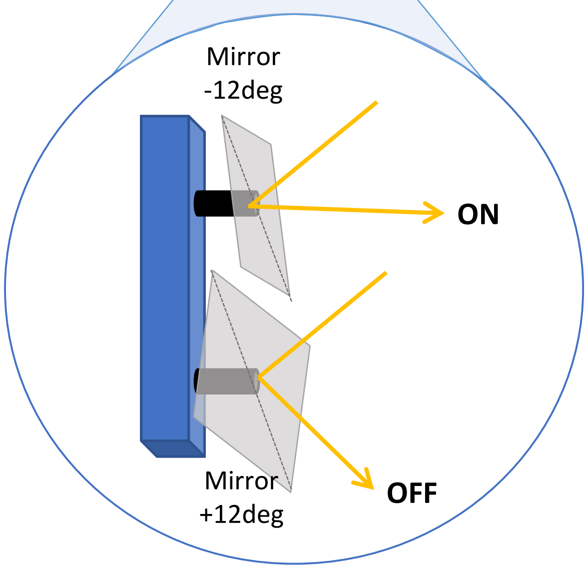

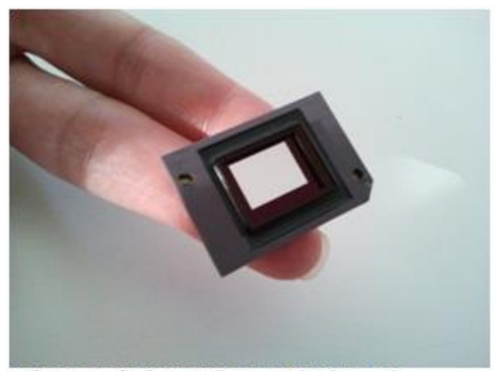

DIGITAL MICRO MIRROR DEVICE (**DMD**)
(**SLM** - Spatial Light Modulator)

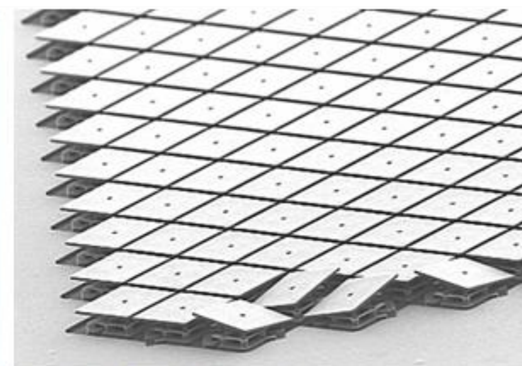

MICRO MIRRORS CLOSE UP

Uniaxial brightness flicker

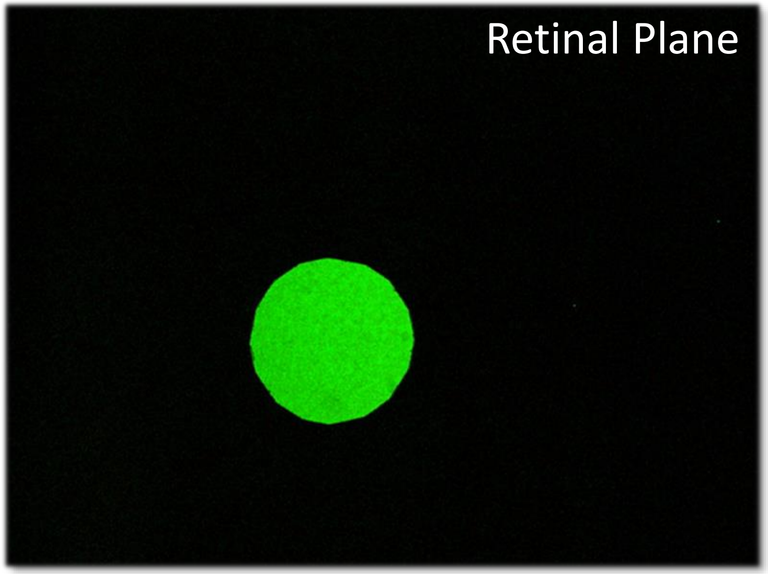

Brighter

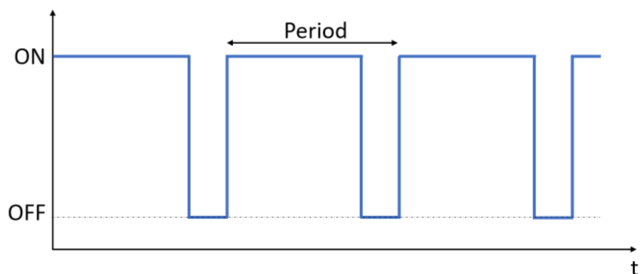

Darker

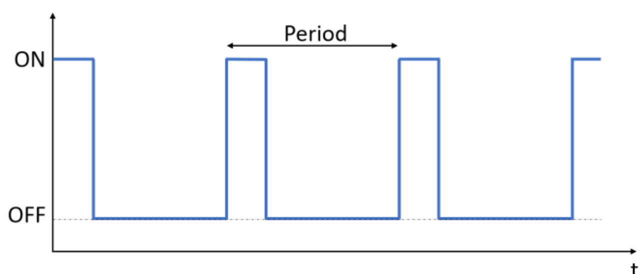

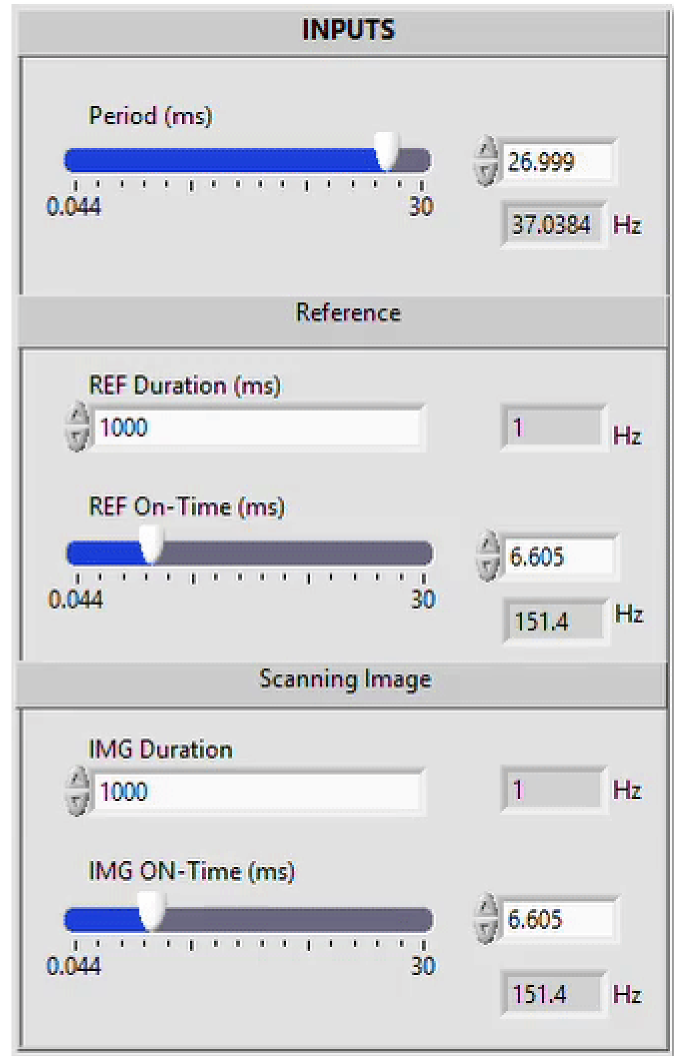

Reduced directionality = large axial length

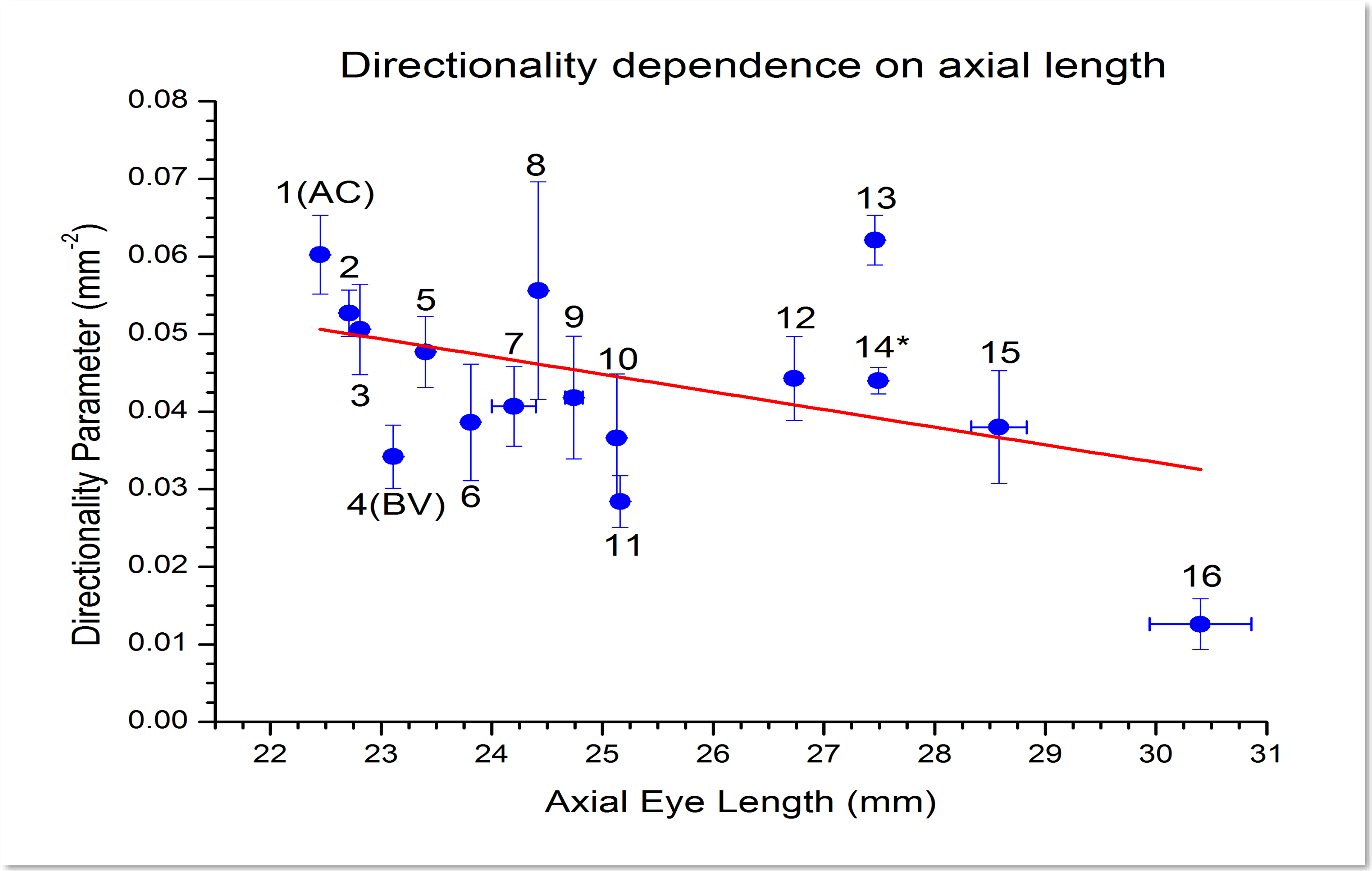

Slope: -0.002 ± 0.001 mm^{-2}
per *mm* axial length
R^2=0.1796

$$\rho_M \simeq (1 + 2Df_E)\rho$$

Accommodation and emmetropization

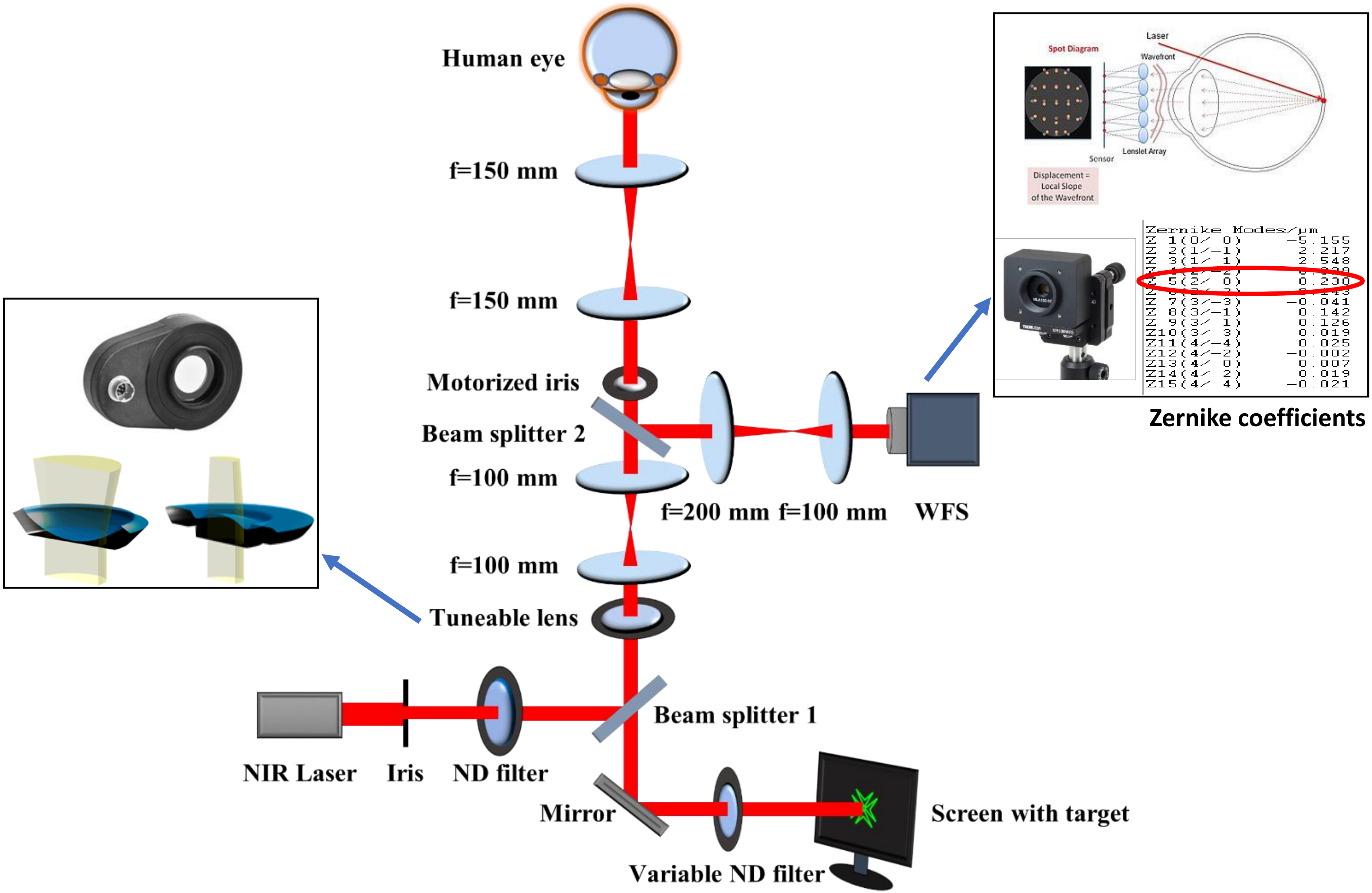

Altered eye growth in animal models

Eye growth can be locally stimulated by local degradation of the retinal image, even after the optic nerve was cut

Thus, the retina has at least the complete machinery to convert image features into growth signals.

***Frank Schaeffel et al**, Ophthalmic Physiol Opt **2013**, 33, 362–367

3-D retina breaks defocus symmetry

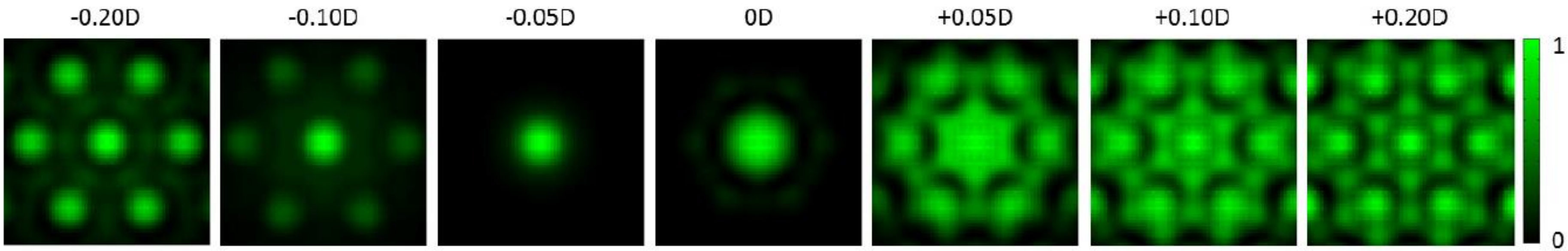

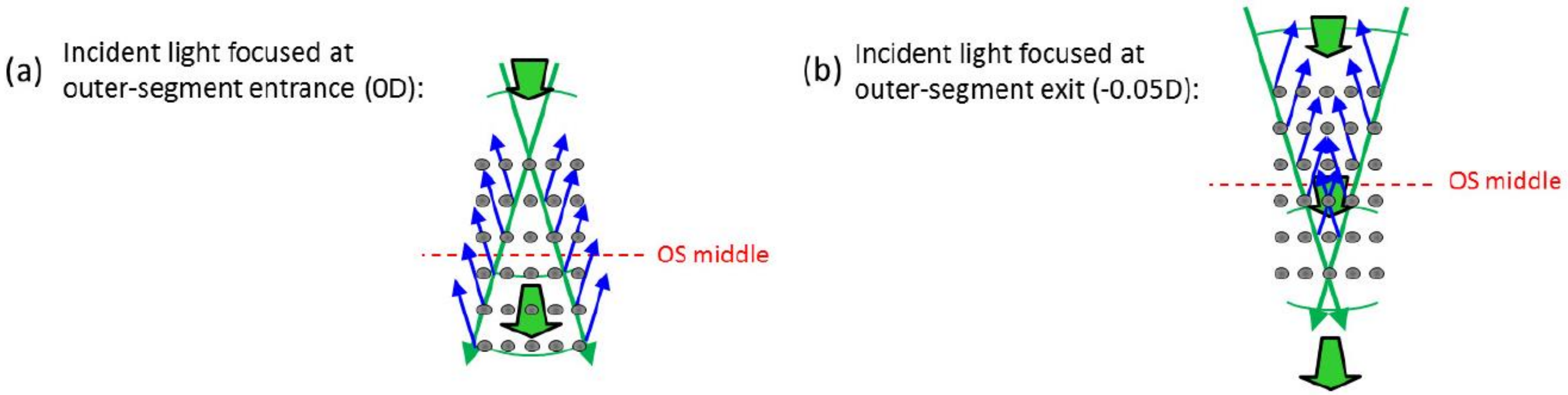

Vohnsen, Biomed. Opt. Express 2014

Temporal response of accommodation

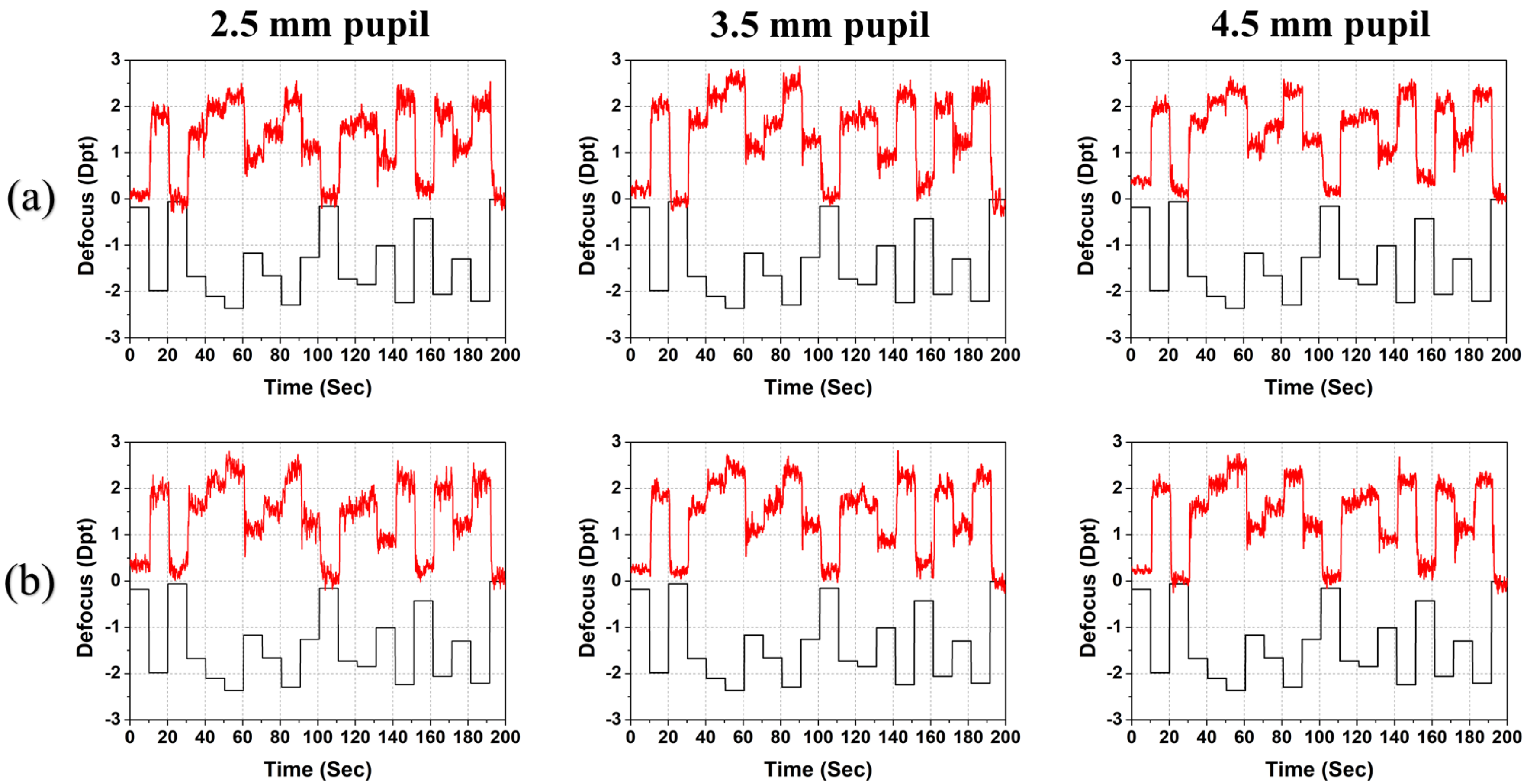

Test subject (29 years)

(a) With and (b) without adjustment of the brightness to compensate changed pupil area

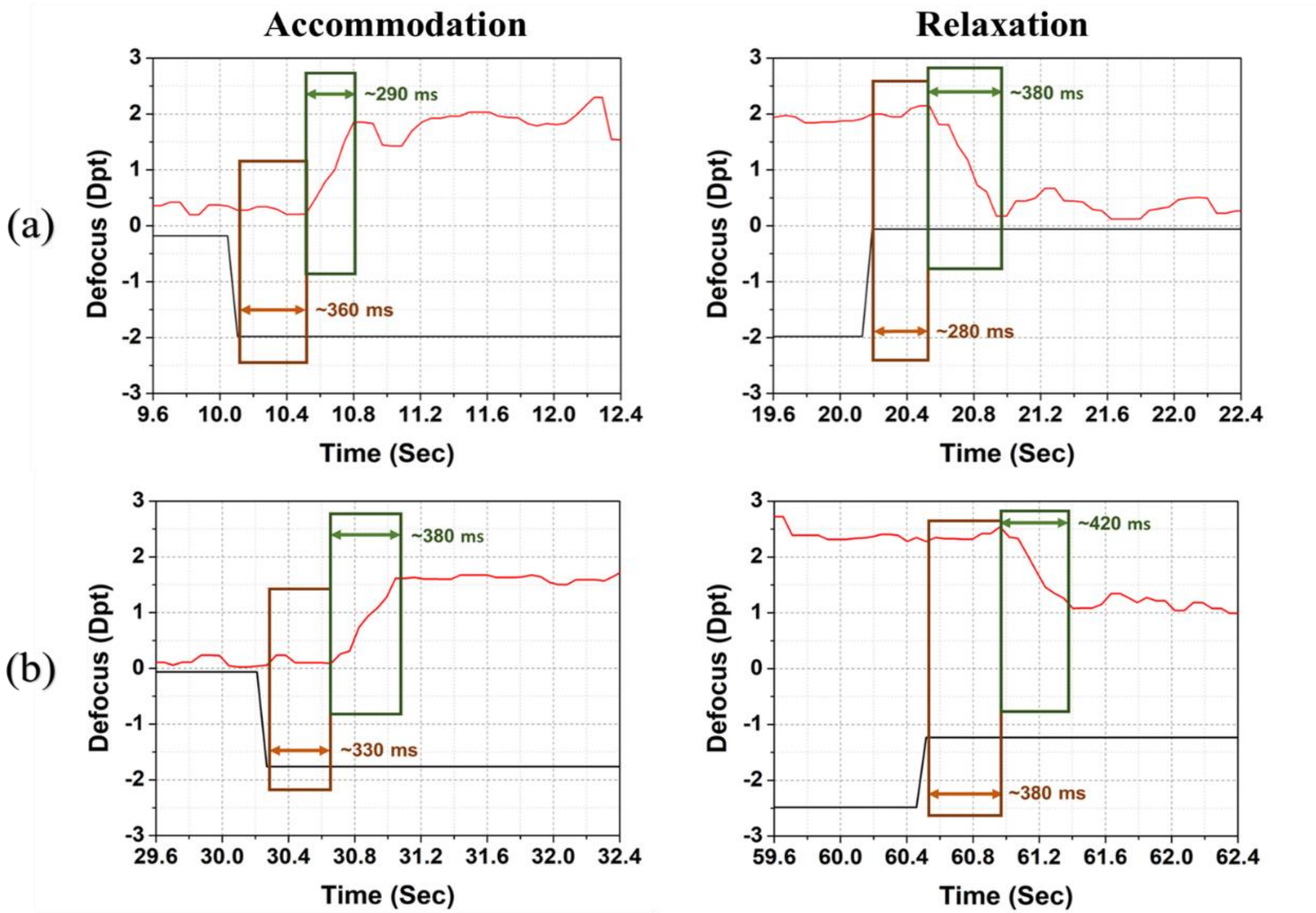

The **reaction time** was found in the range of **300 – 700 ms** and the **response time 200 – 800 ms**

We cannot exclude a neural-triggered response to defocus triggering accommodation

Towards retinal implants…

fighting blindness

Retinitis Pigmentosa (RP) disease

State-of-the-art implant

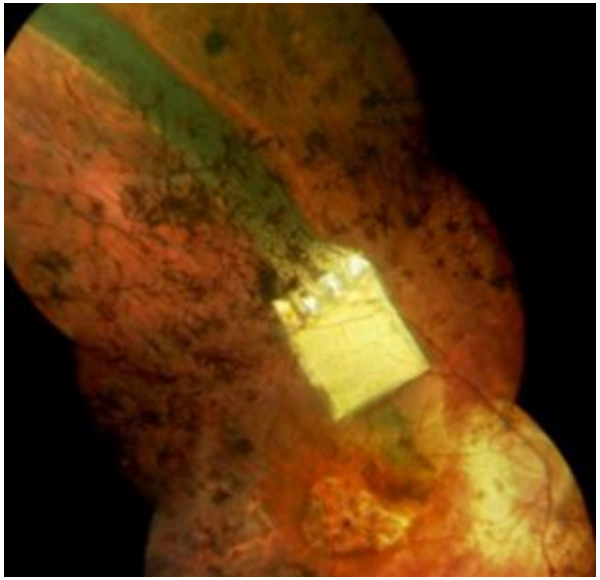

Retinal implant alpha

+

A retinal simulator in 50μm photoresist AZ40XT

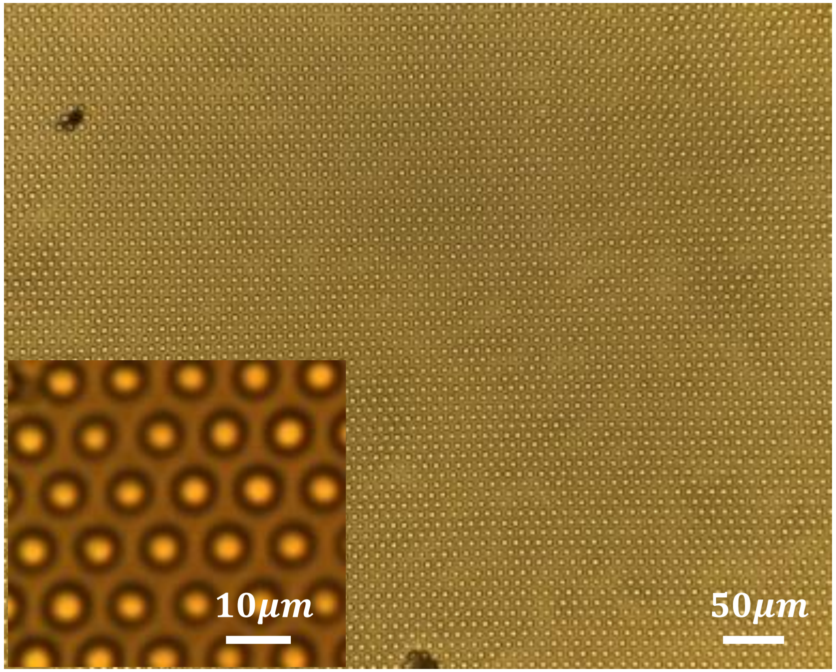

Valente & Vohnsen, Opt. Lett. 2017

Retinal simulator model, angular tuning

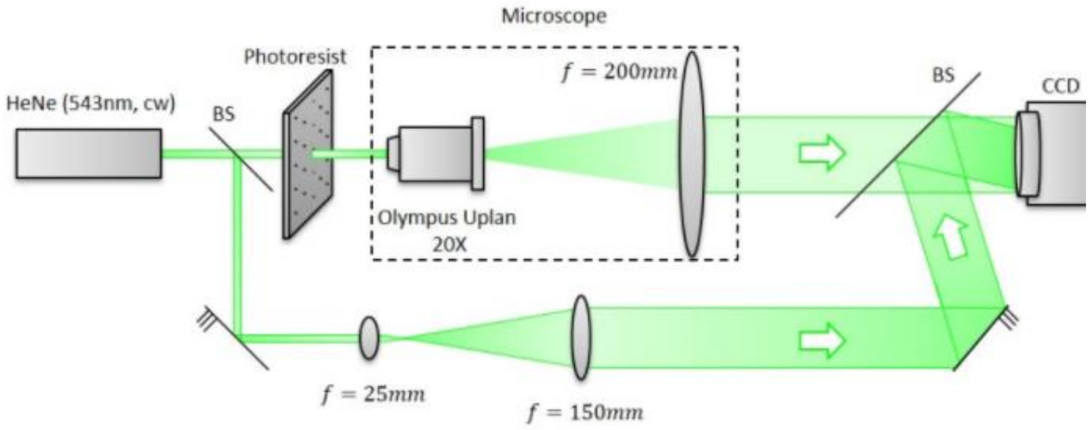

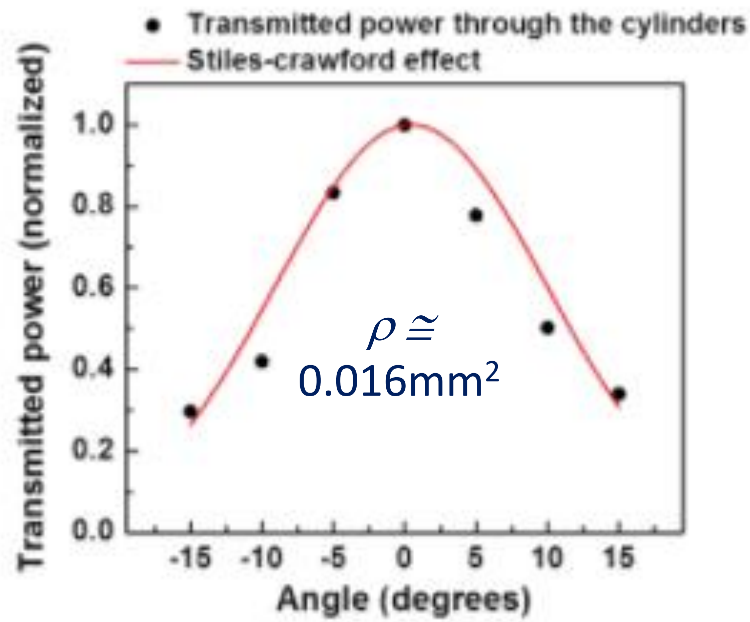

$n_{core} = 1.585$
$n_{cladd} = 1.581$

$d = 5\mu m$

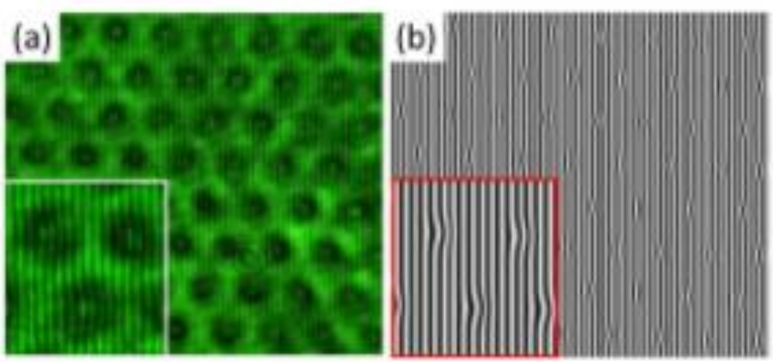

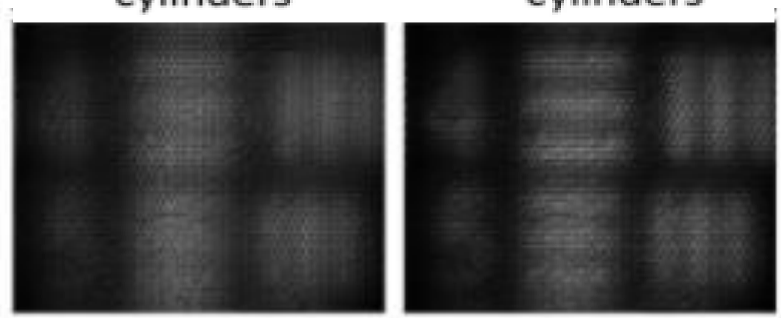

Valente & Vohnsen, Opt. Lett. 2017

Photoresist waveguide array, role of waveguide length

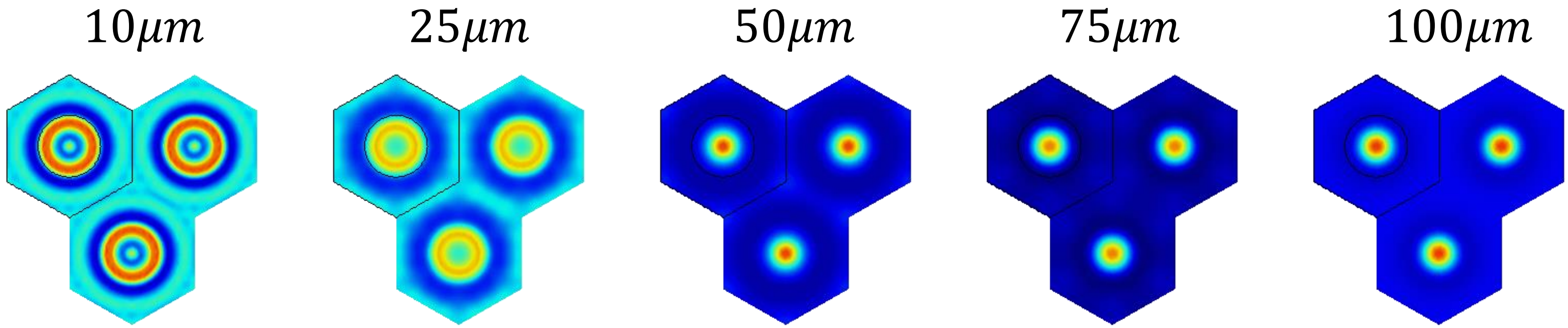

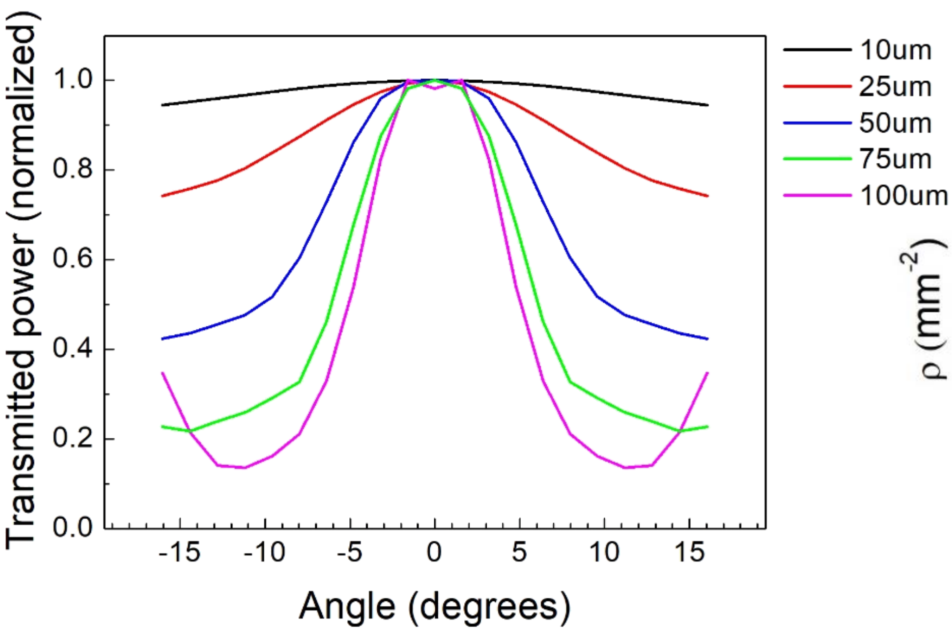

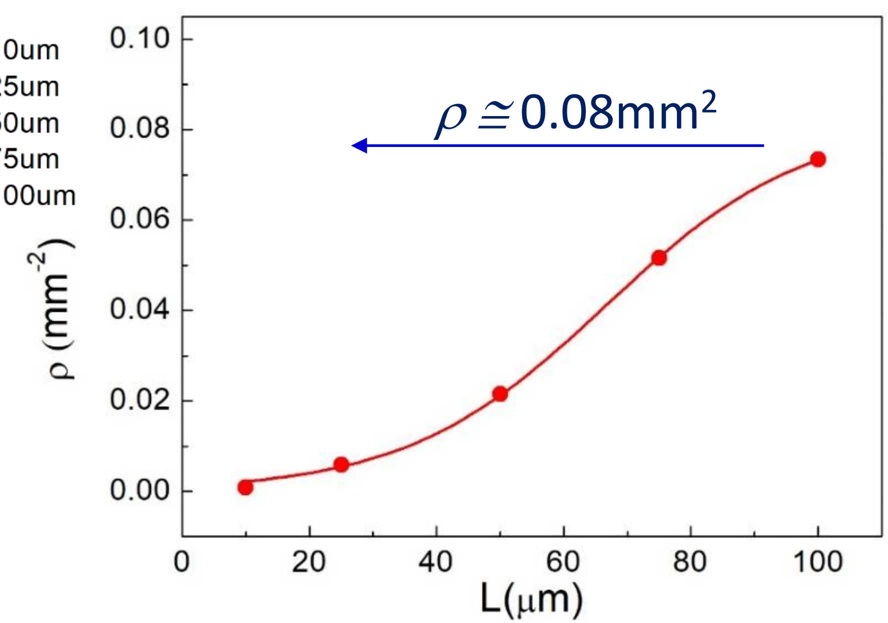

Vision with an implant

Argus II, retinal implant (60 pixels)

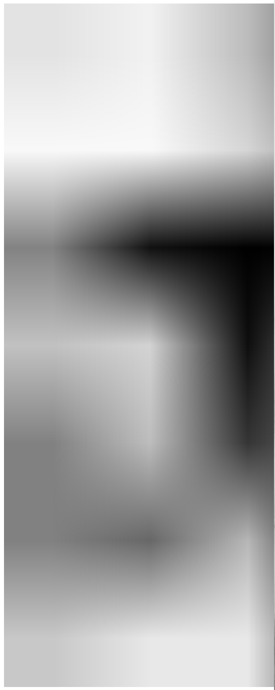

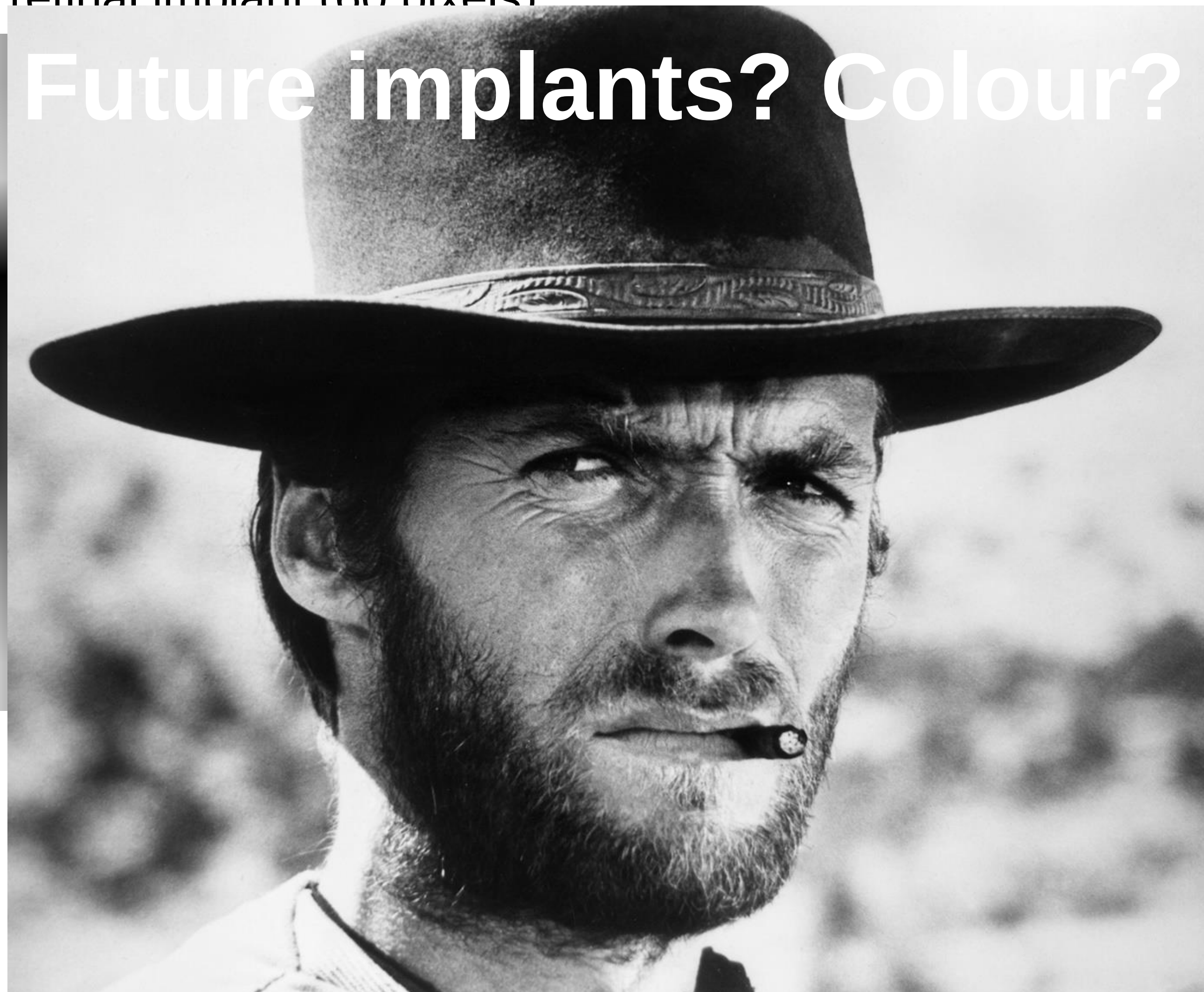

(1500 pixels)

Directionality when imaging photoreceptors

Wave-optics interpretation:

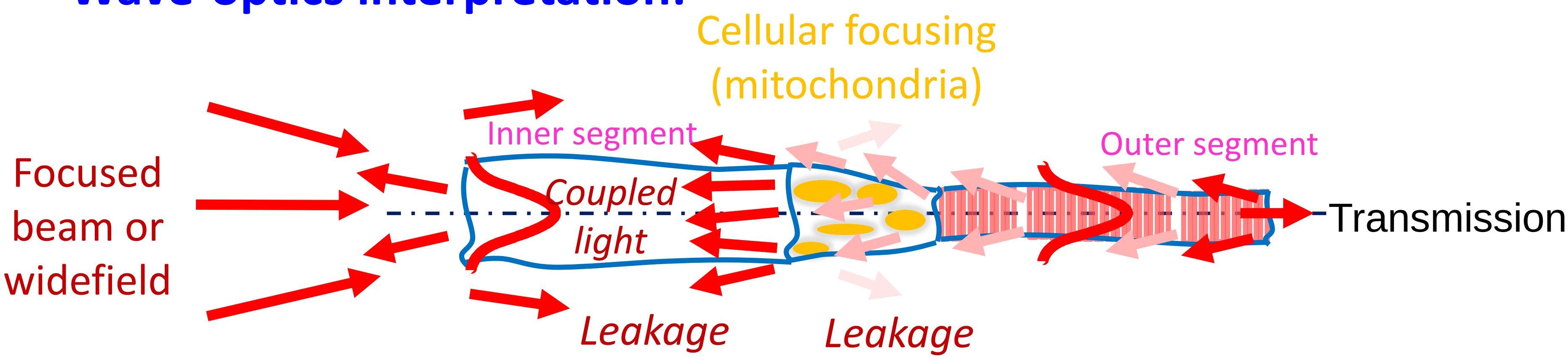

- ❑ Scattering and diffraction from photoreceptors (Vohnsen, BOE 2014)
- ❑ All about refractive index contrast
- ❑ Feature size determines backscattering angle

Problems?

- ➢ Impact of densely packed receptors?
- ➢ Waveguide and interface variations (beyond 8° no TIR)?
- ➢ What *can* be seen, and what *cannot* be seen?

High resolution retinal imaging

In-vivo cone and rod reflection image by courtesy of Alf Dubra (BOE 2011)

Calculated cone mosaic light intensity (no rods included) ARVO (Vohnsen, 2014)

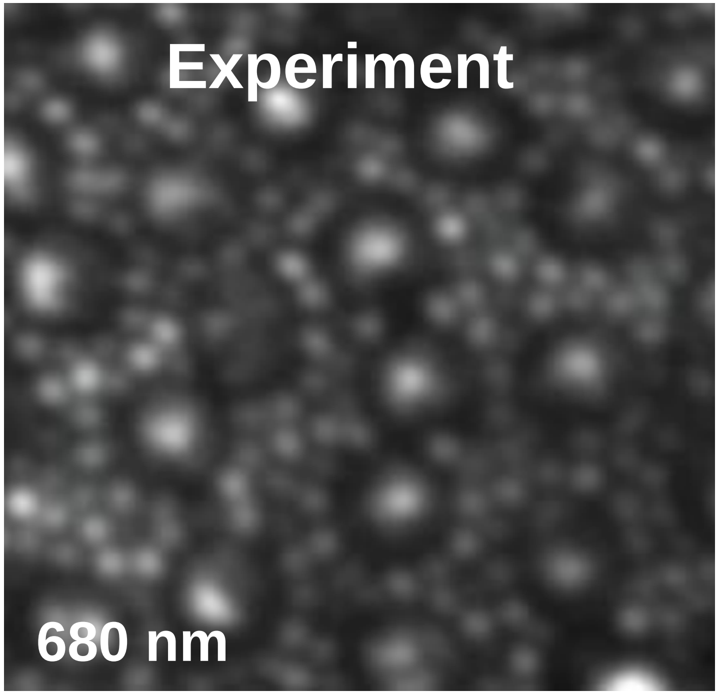

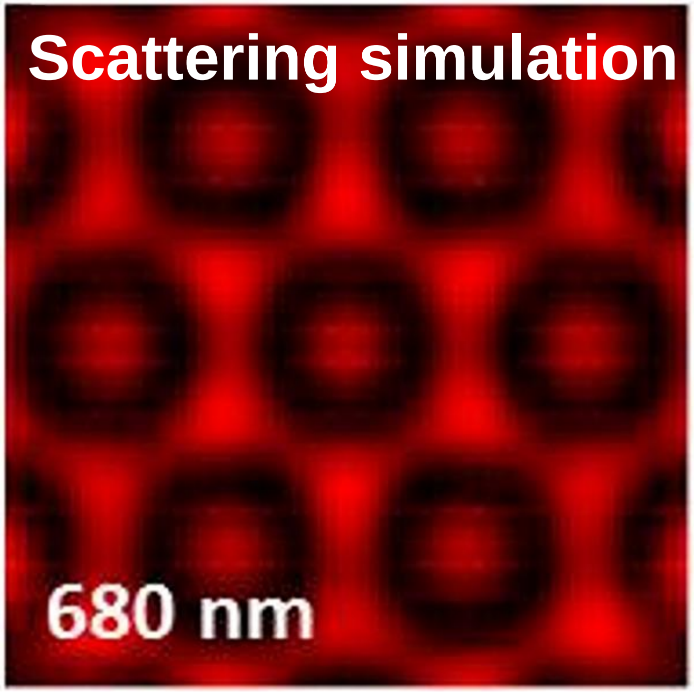

Although images are not on the same scale, notice how the dark rings (that form part of the cones) are seen both experimentally and numerically.

Confocal Scanning Laser Ophthalmoscope

Closed-loop wavefront correction (with a deformable mirror) prior to imaging

Deformable Mirror (DM)
- 140 actuator
- 3.5 micron stroke
- Include 4th-order Zernike
- ∅2.5mm (5mm @eye)

Galvo Scanners
- 12kHz resonant
- 47 fps
- 512 × 512 pixels

Detection (APD)
- 75 micron pinhole
- Video signal
- Avalanche photodiode

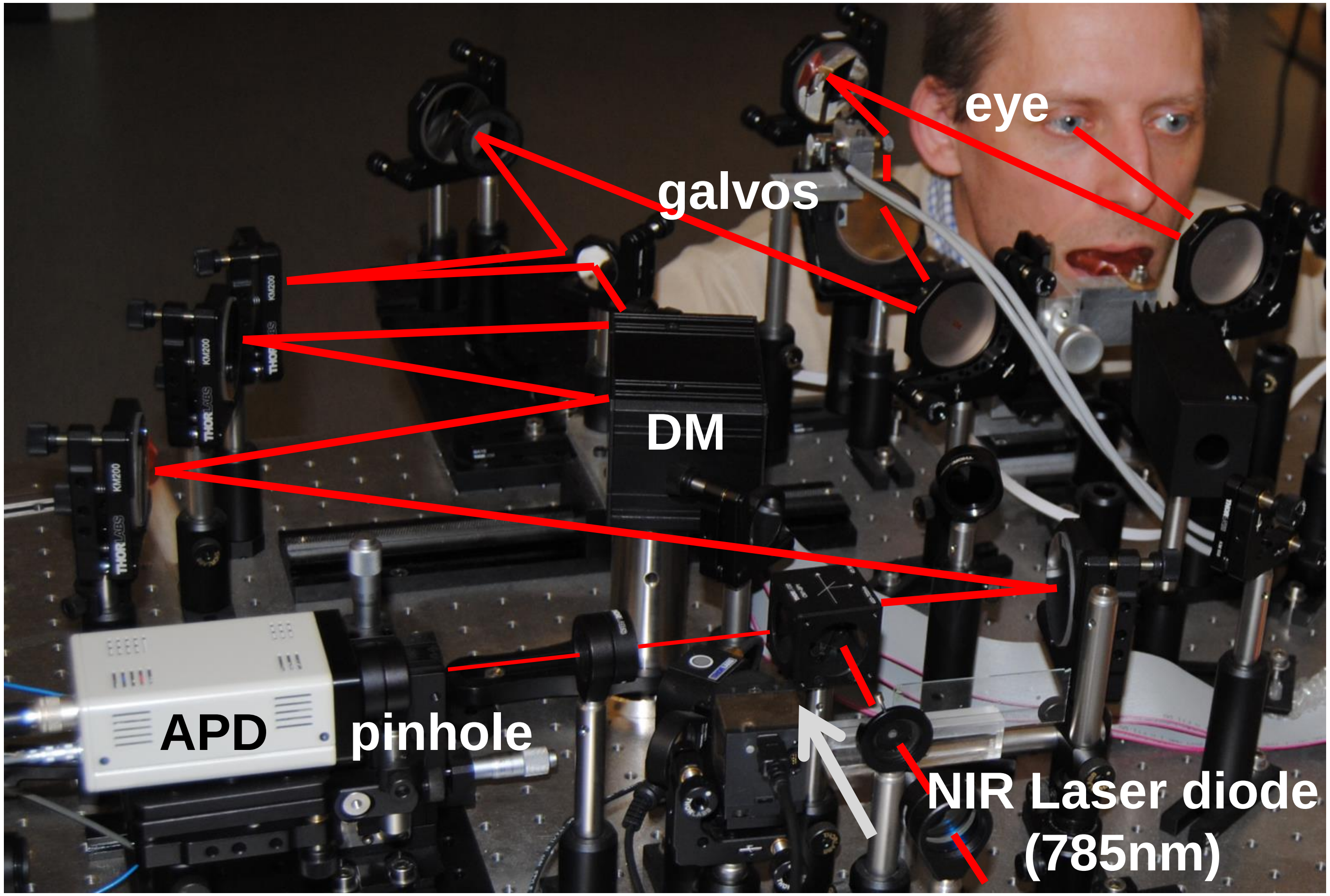

Rativa and Vohnsen, Biomed. Opt. Express 2011

SLO-OSCE analysis with pupil sweep of imaging beam

Fovea vicinity Subject BV Superior parafovea retina

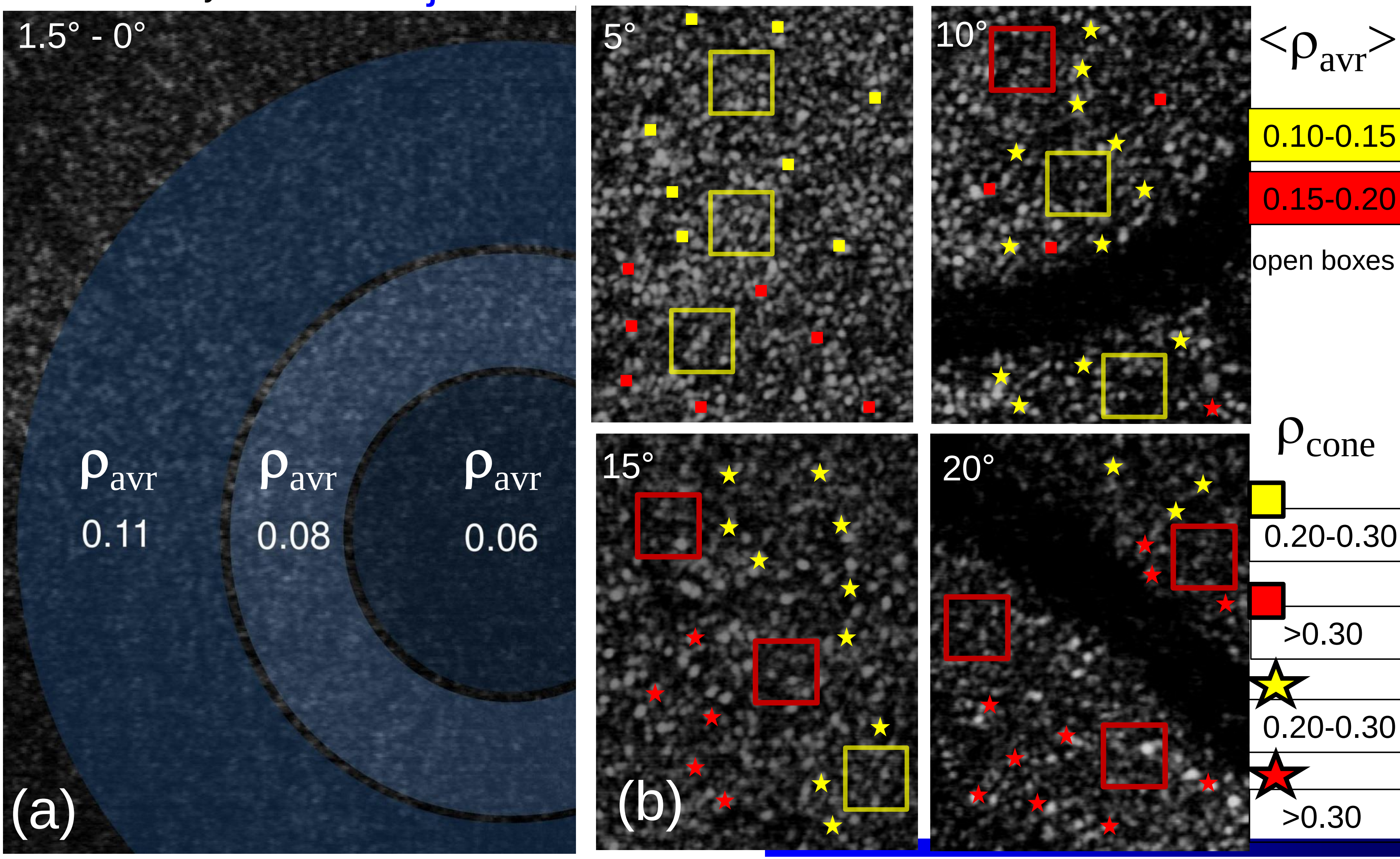

Rativa & Vohnsen BOE 2011

Pupil structuring and directional scattering

Splitting the pupil in sectors for simultaneous retinal imaging at different angles

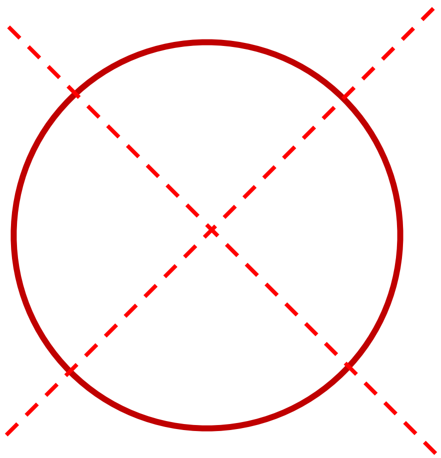

Biomedical Optics Express

Nov. 2018

Differential detection of retinal directionality

SALIHAH QAYSI,[1,*] DENISE VALENTE,[2] AND BRIAN VOHNSEN[1]

Cone pointing analysis with an AO fundus camera (model)

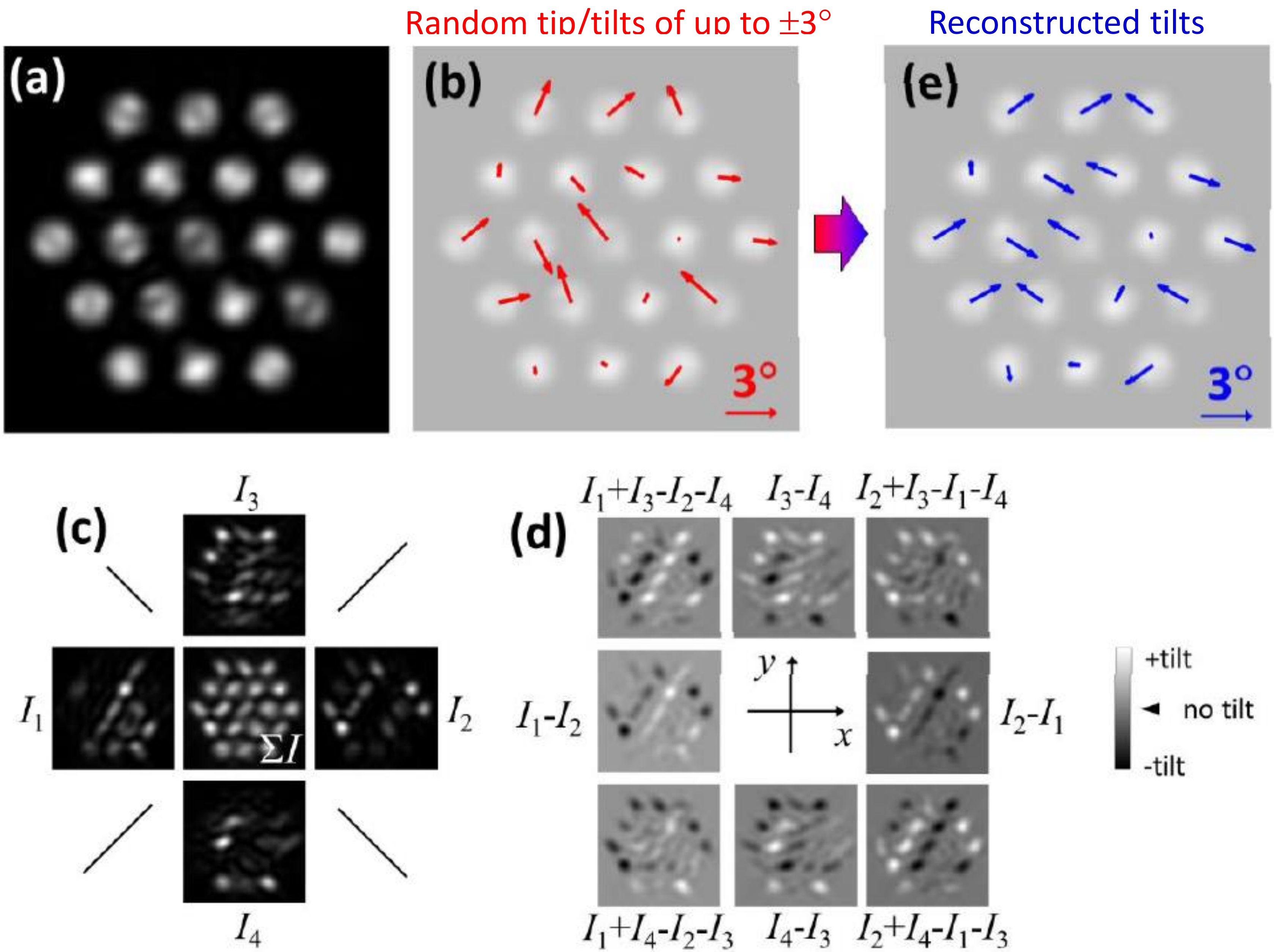

Pupil-sectored retinal images

Images

Difference images

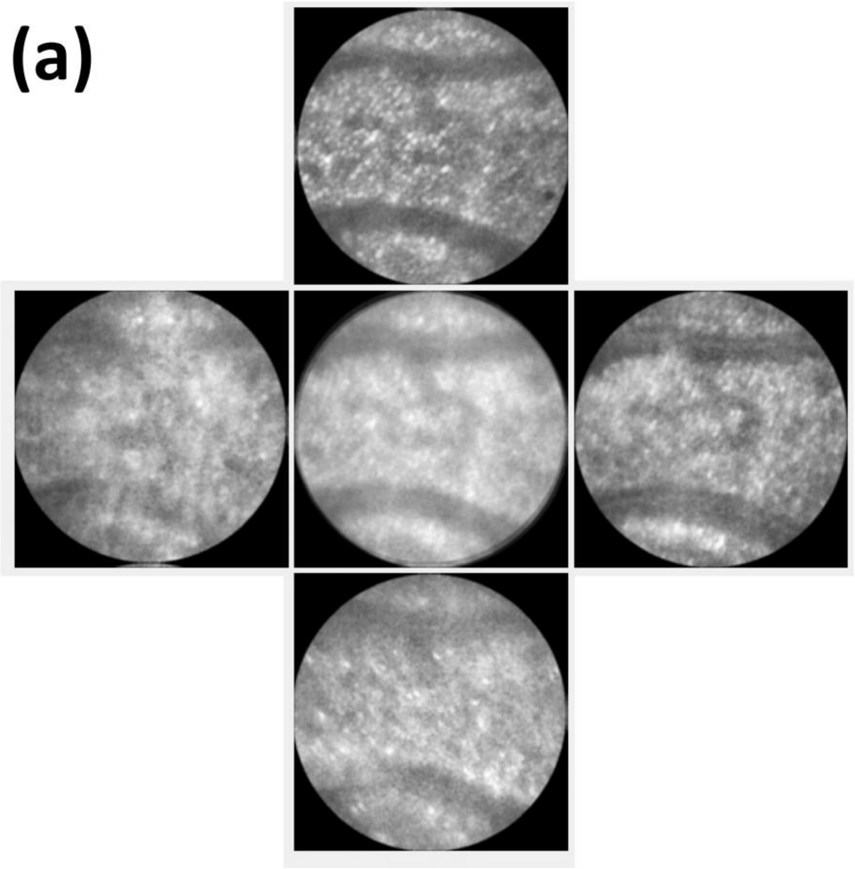

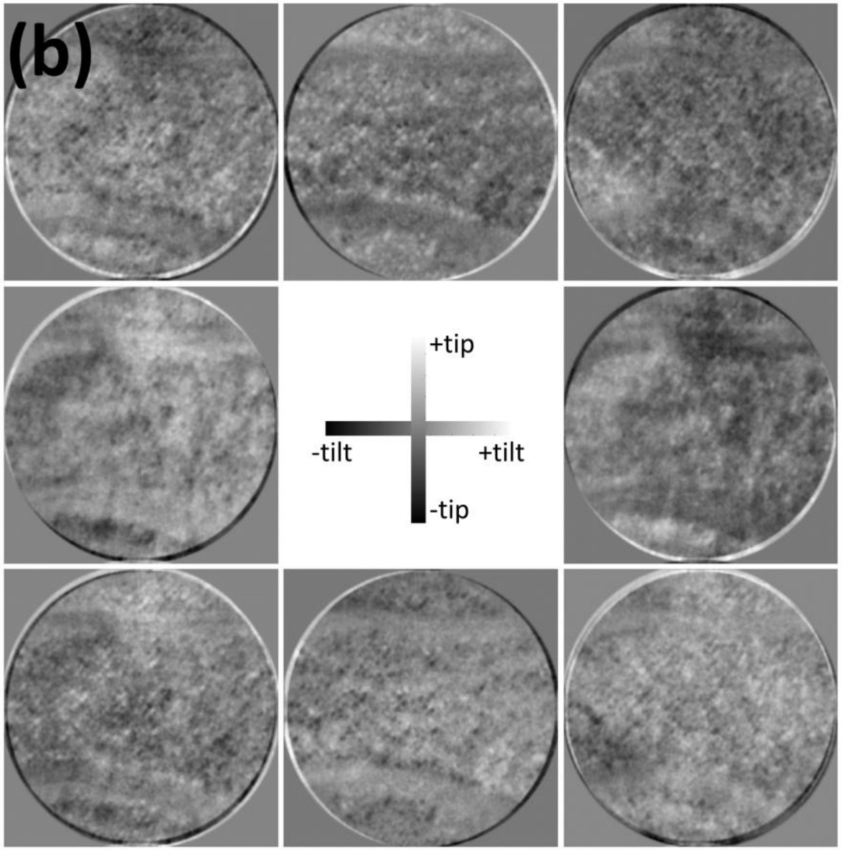

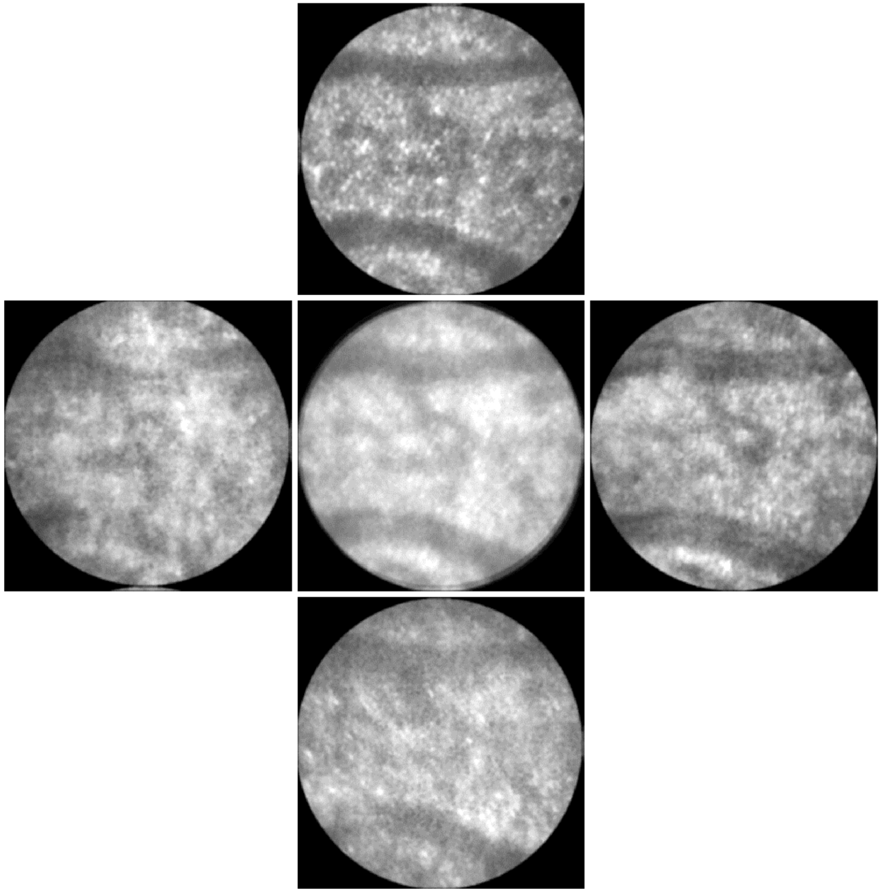

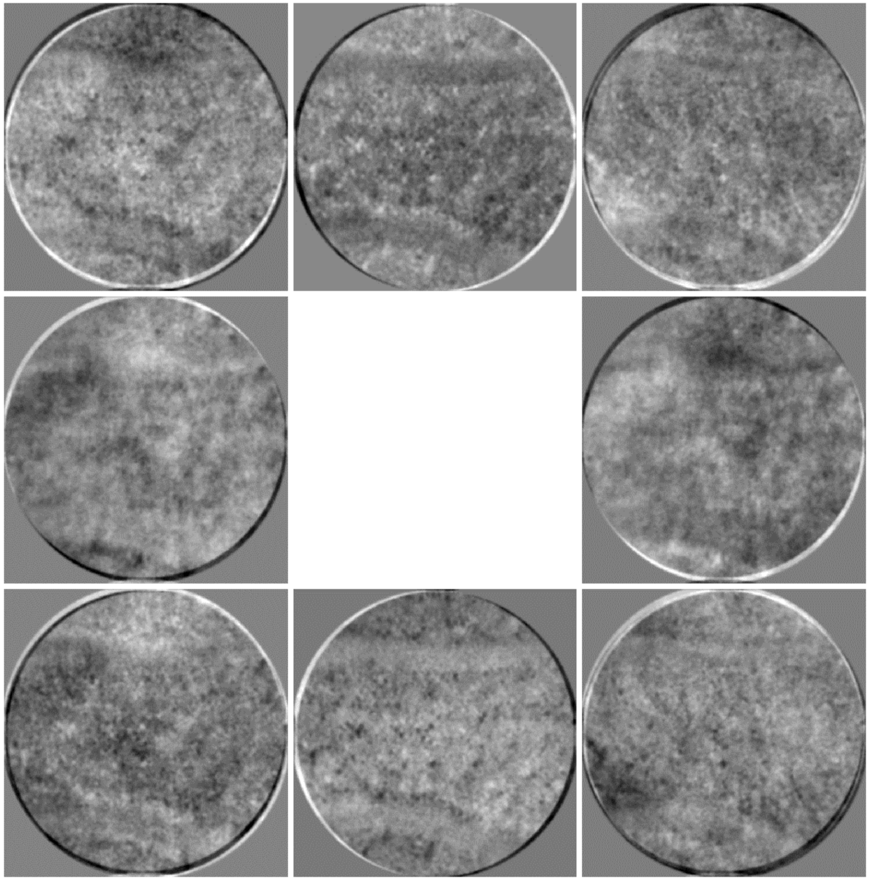

Local inclination vector at each pixel (m,n)

Inclination vector at pixel (m,n)

$$\Delta x_{m,n} = \frac{I_{2,m,n} - I_{1,m,n}}{I_{2,m,n} + I_{1,m,n}} L \quad ; \quad \Delta y_{m,n} = \frac{I_{3,m,n} - I_{4,m,n}}{I_{3,m,n} + I_{4,m,n}} L$$

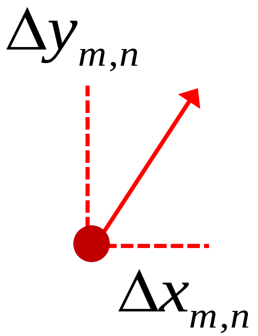

Image inclination metric (N x N pixels)

$$\sigma = \frac{1}{\sqrt{2}N^2} \sum_{n=1}^{N} \sum_{m=1}^{N} \sqrt{\left(\Delta x_{m,n} / L\right)^2 + \left(\Delta y_{m,n} / L\right)^2}$$

Cones with local inclination vectors

Colour-coded parafoveal cone mosaic

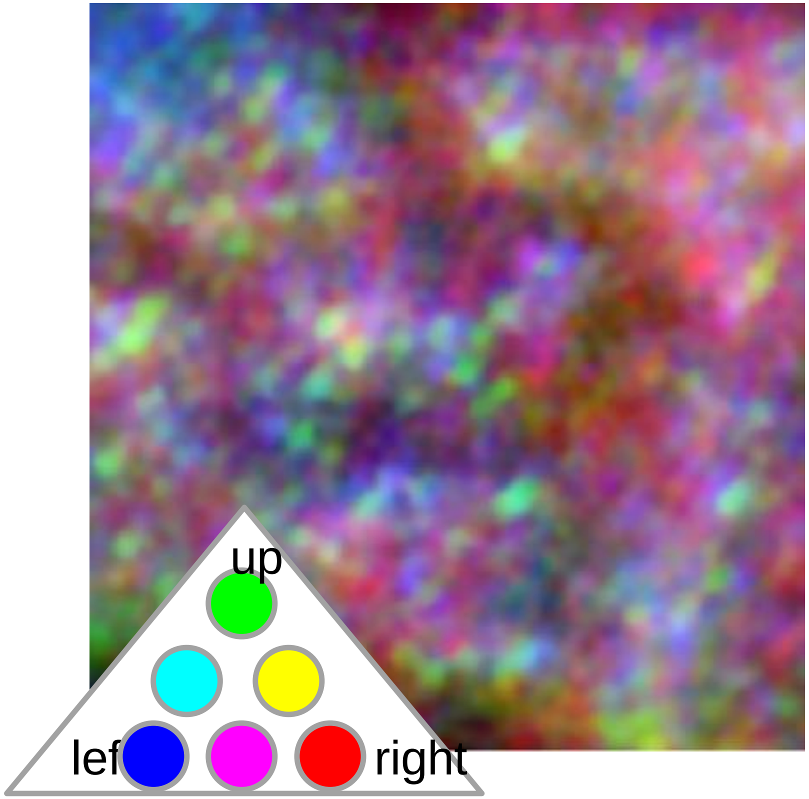

Vector inclination plot

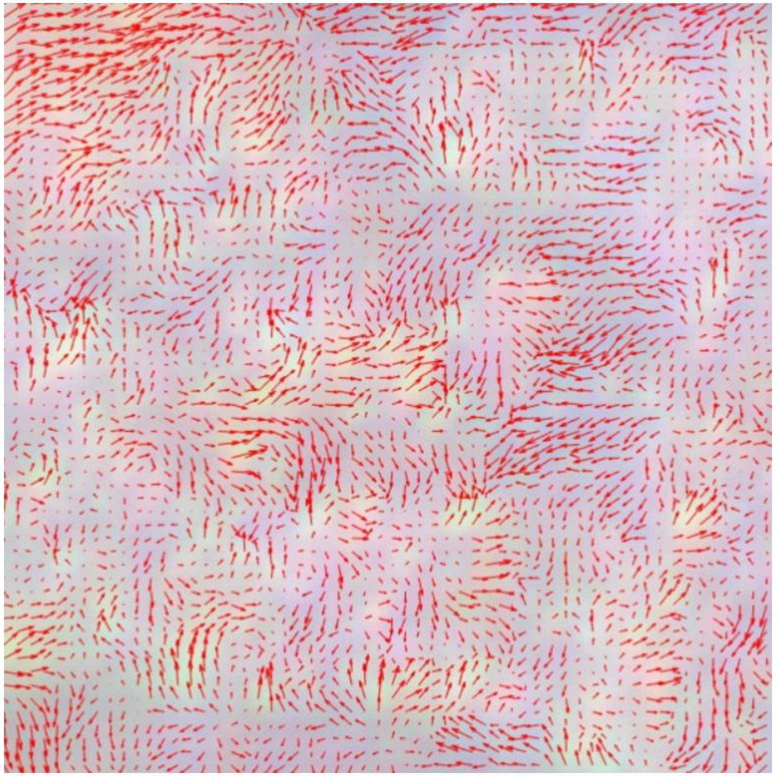

σ = 0.091

Colour coding and inclination near the optic disc

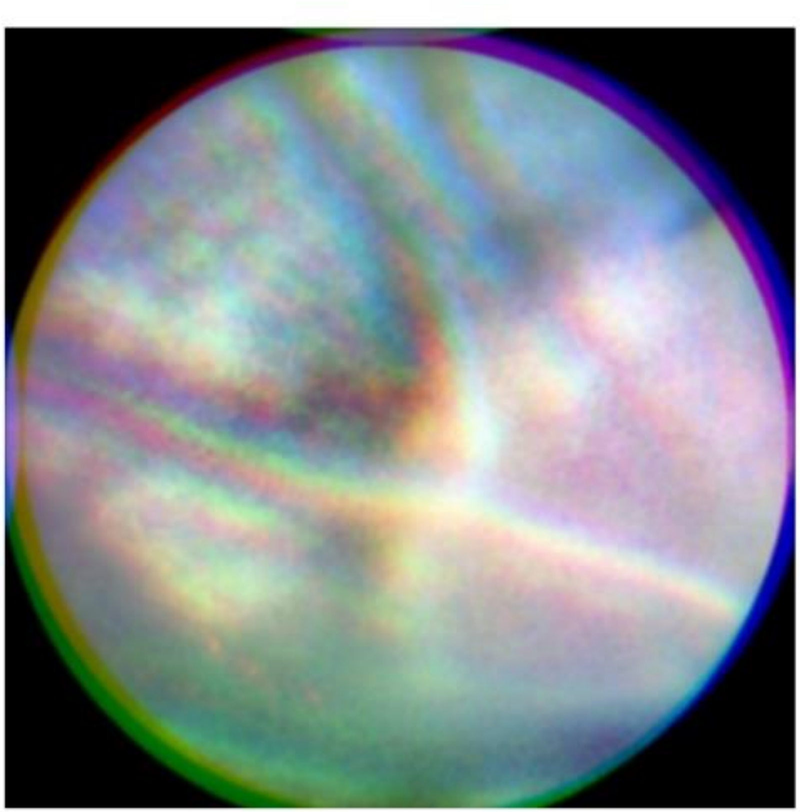

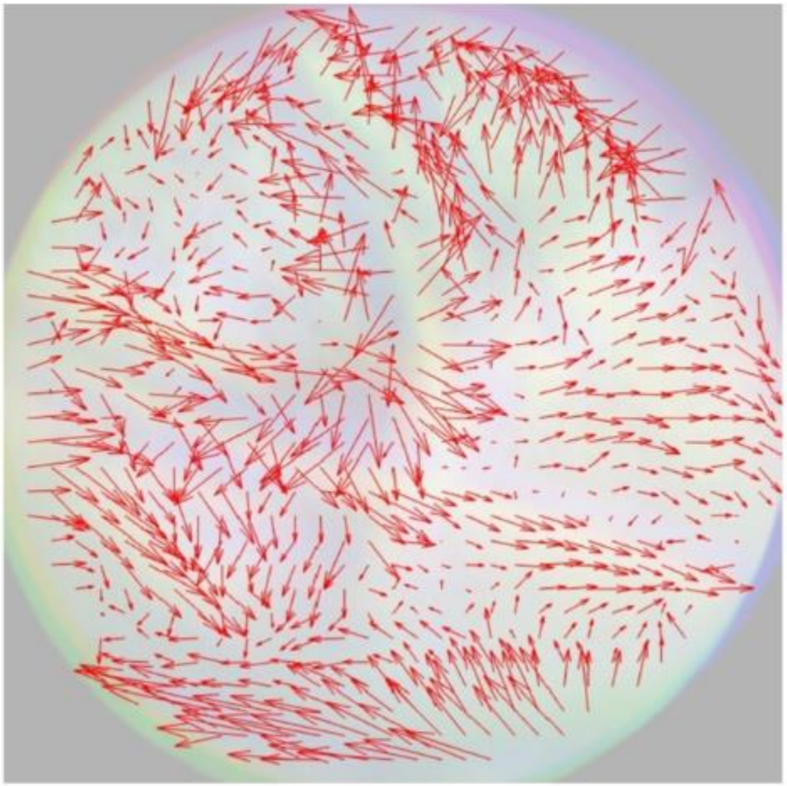

$\sigma = 0.090$

Conclusions

- A volumetric absorption model gives good estimates for the SCE-I and for the integrated Stiles-Crawford effect
- Electromagnetic absorption model gives fair estimates for the SCE-I, and may explain rod directionality due to dense absorption in rhodopsin
- Scattering calculations can produce simulated images that may help interpret experimental results
- Directional retinal scattering can be analysed with differential analysis as demonstrated with an AO-fundus camera

Acknowledgments

Dr. Martin Isaias Rodriguez

Alessandra Carmichael Martins

Denise Valente

Salihah Qaysi

Najnin Sharmin

Prince Sunil Thomas

European Commission

CONACYT

MYFUN

King Abdullah Scholarships Program

SCIENCE WITHOUT BORDERS

ENTERPRISE IRELAND

IRISH RESEARCH COUNCIL
An Chomhairle um Thaighde in Éirinn

brian.vohnsen@ucd.ie

PSF and MTF (mis-)concepts

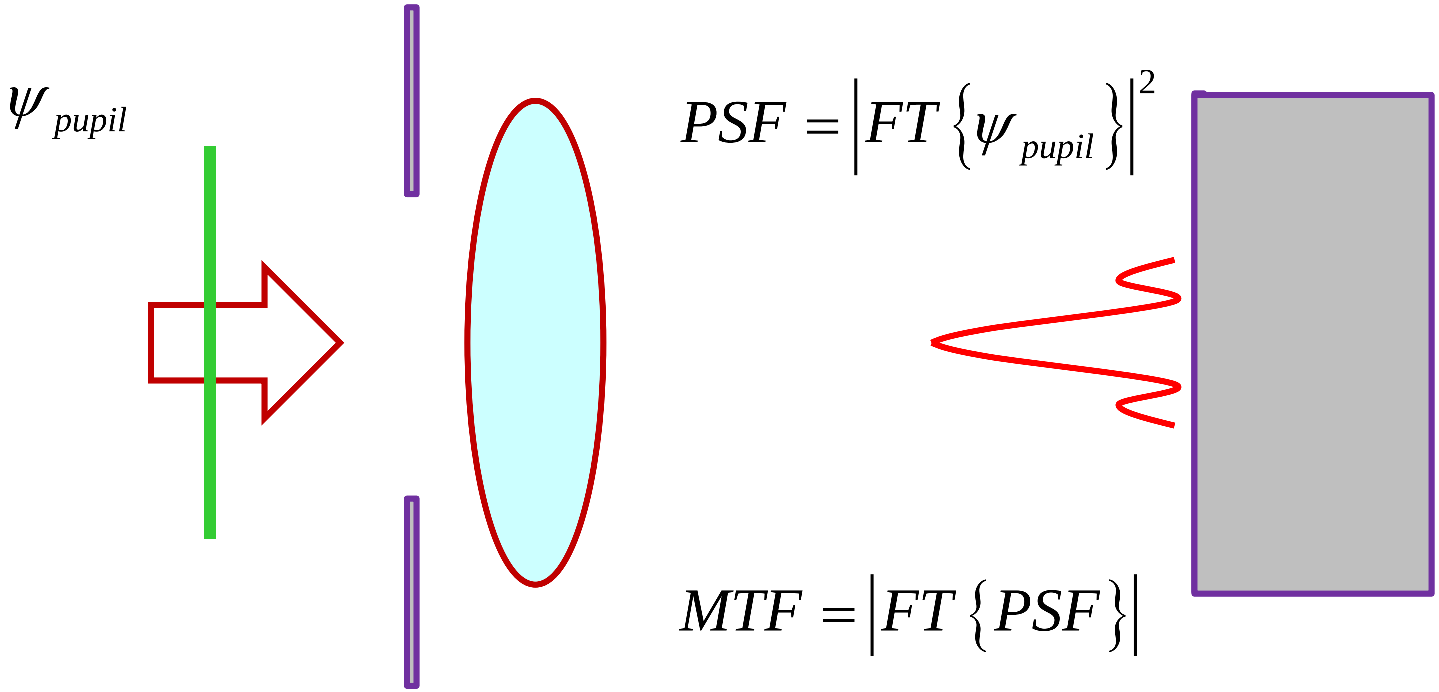

$$PSF = \left| FT\left\{ \psi_{pupil} \right\} \right|^2$$

$$MTF = \left| FT\left\{ PSF \right\} \right|$$

Depth-of-focus $DOF = 8\lambda f^2 / d^2$

…at best these are 1st-order approximations